S-Duct Inlet Design and Experimentation for Small TurboJet Applications - Final Report

- APOP Black Team -
Jacob Bradley, Joshua Melvin, Mac Ramsey, Caleb Robb, Matt Sutterfield, Emerson Williams
Mechanical & Aerospace Engineering, Oklahoma, Stillwater, 74075

This report outlines the process of testing an S-duct inlet for a JetCat P100-RX engine that satisfies the requirements of the 2020-2021 APOP design challenge, as well as the data that accompanied this testing. Through the use of a moment arm test stand, the data for thrust could be quickly tested for. Experimental results for pressure recovery were evaluated utilizing a static pressure ring and Kiel probes for total pressure measurement. The data was then processed and reported in the form seen in this report. Although the design is likely to change, the first iteration showed promising results, with a thrust difference of 0.1% and a pressure recovery value of 99.57%. The pressure recovery can be directly compared to the CFD results that showed a pressure recovery value of about 99.8% at full rpm. In addition, the SFC value only increased by about 1% when the inlet was installed. After these results varied so little, an inlet with a smaller build volume was created to take advantage of this difference. However, the newer iteration was not able to be tested because of technical issues associated with the engine and testing equipment. It is assumed that this inlet would have produced results comparable to the CFD results, which showed a pressure recovery of 99.3%. One final iteration was completed by reducing the axial length by half an inch. The overall recovery was seen to be 99.09% in this iteration. The team saw a 0.23% frictional loss from the first iteration's experimental testing, and they do not expect that result to increase substantially; this iteration is deemed very likely to succeed. The team is satisfied with the promising recovery results, especially when compared to the small model volume. Further experimental testing is recommended as well as continued iteration.

I. Nomenclature

F	=	uninstalled thrust
$\dot{m}$	=	mass flow rate of air
g_c	=	proportionality constant
c_p	=	constant pressure specific heat
CFD	=	computational fluid dynamics
γ	=	specific heat ratio
P_t	=	total pressure
P	=	static pressure
T_t	=	total temperature
M	=	Mach Number
π	=	total pressure ratio
η	=	component efficiency
f	=	fuel/air ratio
MFP	=	mass flow parameter
FEA	=	finite element analysis
PPE	=	personal protective equipment
$TSFC$	=	thrust specific fuel consumption
WDM	=	weighted decision matrix
$AFRL$	=	Air Force Research Laboratory
$OSHA$	=	Occupational Safety and Health Administration

II. Introduction

This paper presents the Aerospace Propulsion Outreach Program (APOP) design competition for 2020-2021 which tasks students to develop an S-Duct inlet for the JetCat P100-RX. This inlet will allow for future engine airframe integration, as engines are typically mounted along the centerline of an airframe with a ducted inlet that extends to the capture area. For this project, the new inlet design transports flow from a single capture area that is 6 inches from the top of the capture area to the centerline of the JetCat engine. The AFLR provided Fig. 1 shows a representation of the vertical distance between the engine centerline and the inlet capture area.

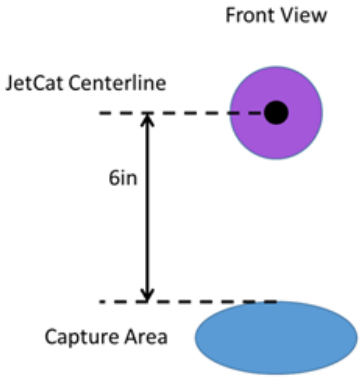

Figure 1: Inlet Offset Requirement

The main goal of this inlet design will be to minimize the performance losses of the JetCat engine. In order to achieve this, the inlet will minimize total pressure losses and distortion of the airflow entering the engine. By doing this, the maximum thrust and thrust specific fuel consumption (TSFC) will be as close as possible to reference operating conditions. These reference conditions will be measured by way of engine tests with the Air Force Research Laboratory's (AFRL) bell mouth inlet design attached to the JetCat engine. The S-duct inlet will then be attached and the engine's performance will be recorded and compared. These tests will be conducted on the AFRL test stand. An example of this process can be seen below in Fig. 2.

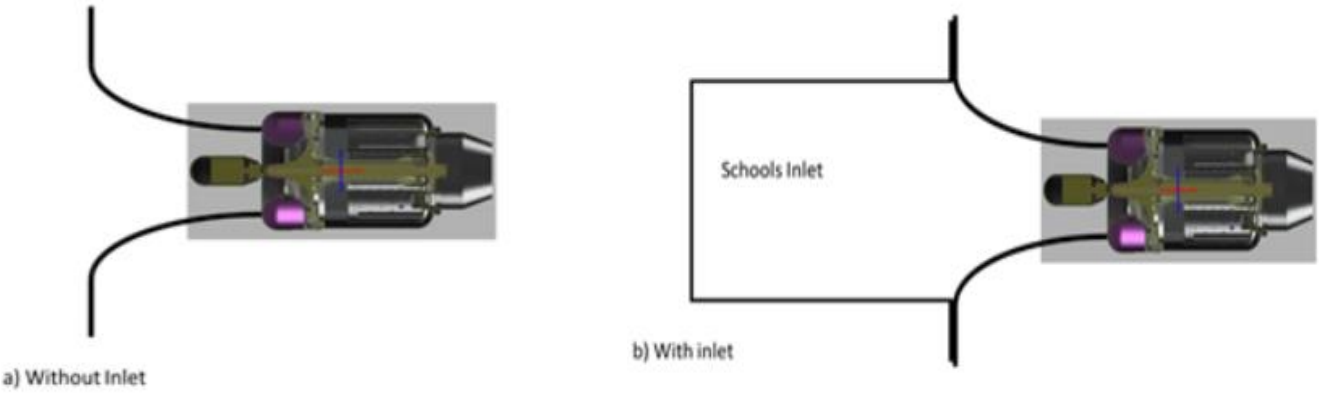

Figure 2: Inlet Testing Method

The S-duct inlet performance goals can be broken down into primary and secondary objectives. No matter the inlet design, the primary objectives should be achieved in order for this project to be a success. The secondary criteria are additional goals that will ultimately distinguish successful inlets from each other. The primary and secondary goals criteria can be seen below:

Primary objectives

- a total pressure recovery that is greater than or equal to 98%
- a maximum thrust decrement of less than 5%
- a TSFC decrement of less than 5%.

Secondary objectives

- minimization of the axial inlet length
- minimization of total inlet volume.

The minimization of the inlet size is advantageous, as this allows for additional payload, fuel, or structure that will improve the mission capabilities of an airframe designed around this engine configuration.

III. Background

A reliable and accurate form of measuring engine performance is critical to assessing influence of an inlet design. To do this, a moment arm thrust stand was designed to accomplish this. A representation of this test stand can be seen in Figure 3. As seen below, the Jetcat engine is mounted toward the top of the mount away from the table in order to mitigate flow effects from the surroundings. The mount itself is constructed from aluminum T-slotted rails. This frame is then fixed to the table through the use of mounted ball bearings. This configuration will allow the frame to rotate about the bearings with minimum frictional losses to measure thrust. A load cell is placed in front of the bearings on another moment arm that is rigidly attached to the engine arm in order to measure the resultant force produced when the engine is activated.

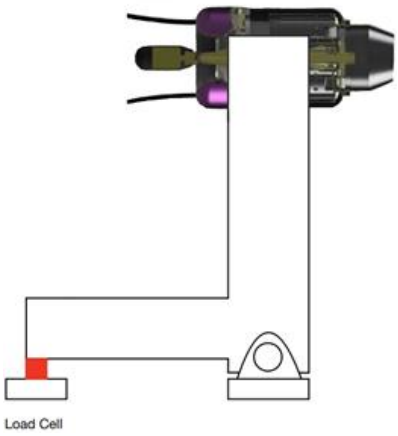

Figure 3: Test Stand Representation

This design was chosen as it is simple, efficient, quick to build, and can easily be modified to accommodate various components. This is due to the way that this configuration measures the thrust produced by the engine. An idealization of the forces present on the test stand can be seen above in Figure 4. The "Reaction Force" will be the force seen by the load cell. By summing the moments about point A, which is the axis of rotation due to the mounted bearings, the thrust can be calculated through the use of equation 1.

$$T = \frac{R_y * L_C}{L_g} \quad \textbf{(1)}$$

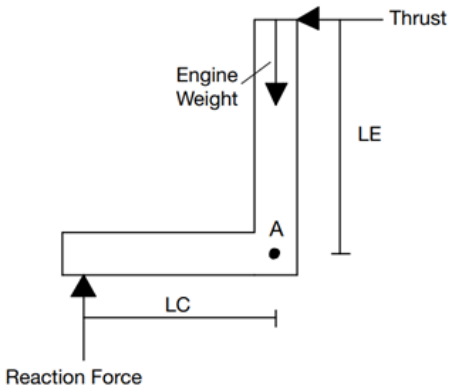

Figure 4: Test Stand Moment Forces

This equation assumes that the weight of the engine is exactly vertical from point A. Naturally, during the installation of the various inlets, the center of gravity of the engine will change, which will affect the load cell reading. These inaccuracies will be taken into account through careful calibration. To account for the difference in center of gravities, the load cell will be tarred to zero with each new inlet that is tested. This will provide accurate and reliable thrust data to compare between various inlet tests.

As it can also be seen in equation 1, by varying the lengths of the moment arms, a variety of load cells with different ratings can be utilized. This will provide a great benefit in the case that any components break or fail, simply changing the configuration will allow for a straightforward replacement process that will minimize delays.

A. Mass Flow Parameter (MFP)

In order to optimize the inlet design, a variety of inlet geometries were tested. Through the use of mass flow parameter (MFP) which is defined in equation 2, the optimal area of these different geometries was able to be determined. Since MFP is a function of the Mach number and the specific heat ratio of the air γ, equation 2 could be rearranged to solve for area. Testing on the engine yielded an optimal mass flow rate to be used for this calculation. With this information, the geometry of the inlet was varied in an attempt to optimize flow properties desired by AFRL and balance secondary criteria.

$$MFP = \frac{m}{A} * \frac{\sqrt{T_T}}{P_T} \quad \textbf{(2)}$$

B. Fanno Flow

Fanno flow analysis was used to understand the effect that friction has on the performance of the designed inlet. For the fanno flow analysis, it was assumed that the curvature of the S-duct inlet contributes no additional losses for the analysis and was treated as a straight pipe. The knowns in the analysis were the Mach number at the inlet face, the ratio of specific heat of air, and an approximated friction factor of the 3D printed PEEK material that the final inlet will be printed with. With the desired percent pressure recovery of 98% known, an optimum length over diameter ratio for the inlet was determined. The L/D ratio was then utilized in the design process when choosing the capture area and axial length of the designed inlet. The Fanno flow results demonstrated the length needed to accelerate the flow from the first Mach Number to the second using boundary layer nozzle effects. This length was useful in showing the magnitude of the effects of Fanno flow, for example a very large length to diameter ratio would show that the effects of Fanno flow are fairly negligible. The key Fanno Flow equations used in calculations can be seen below.

$$\frac{4fL^*}{D} = \frac{1-M^2}{\gamma M^2} + \frac{(\gamma+1)}{2\gamma} ln\left(\frac{(\gamma+1)M^2}{2+(\gamma-1)M^2}\right) \quad \textbf{(3)}$$

$$\frac{P_0}{P_0^*} = \frac{1}{M}\left(\frac{2+(\gamma-1)M^2}{(\gamma+1)}\right)^{\frac{(\gamma+1)}{2(\gamma-1)}} \quad \textbf{(4)}$$

Due to the various assumptions built into the Fanno flow equations, the values obtained are used for preliminary estimations as opposed to final results. This analysis was mainly used to check the pressure recovery to ensure the pressure would not dip below the ninety-eight percent minimum put in place by AFRL. Using this minimum, an optimal length to diameter ratio could be found. In addition, the current frictional effects could also be tested for the current concept. This was done by finding the average diameter and using this to find the length of straight pipe needed to accelerate the flow using boundary layer effects. The length of inlet needed to reach this second Mach Number was found to be very large, suggesting the effects to be negligible.

There are a variety of assumptions associated with Fanno flow analysis that have repercussions on the results. The flow must be one dimensional, steady state, adiabatic flow. In addition, the flow must be travelling through a straight duct, leading to geometric inconsistencies between the requirements of the inlet and the analysis. In addition, the Fanno flow analysis also has a friction factor assumption. Since the geometry is very different for the s-duct inlet than a straight duct, there is a chance this assumption could lead to results that are not representative of reality.

C. Computational Fluid Dynamics

In order to find general trends for the various inlet design parameters, CFD analysis was utilized. It is important to note that CFD was a major factor in the design of each inlet. The analysis completed using this system was a driving factor throughout much of the process. Observations of pressure and the state of the flow were the primary functions in conducting the CFD analysis. The pressure, being an important indicator of flow quality and a scoring criteria, and although there is a two percent pressure loss buffer, it was decided that to be safe the pressure recovery shown using CFD should be above ninety-nine percent. This was a trend to be followed until further pressure testing could be done. Once the reality-theoretical difference could be found, new inlet concepts could be created, ideally consisting of models with minimal volume and axial length. The models which contain the least volume can only be attained if the pressure recovery is still well above ninety-eight percent in the experimental data. The other function of CFD is the flow distortion. Using the software, there can be more visual evidence as to how the flow is moving through the inlet. With this known, mitigation plans can be put in place to reduce separation and increase the quality of the flow. A big way to mitigate much of the separation is through surface roughness. Areas that seem to be prone to separation can be intentionally more rough than other areas in the inside of the inlet so that the flow gains more energy and stays attached for longer.

Another use of CFD is the ability to test different conditions quickly. While trying to test different air speeds experimentally can mean waiting for the perfect conditions, CFD allows for quick iteration using these conditions. This ease of changing the entrance conditions is useful as it allows for testing to see how well the current design works at other conditions. These could include conditions closer to those seen during flight or just a range of airspeeds and pressures that could be closer to those seen in testing locations. Predictions such as these are useful in that, even though they are not perfectly representative of reality, trends still exist and can be used to create an inlet that meets the design objectives.

The concept of flight conditions is also being discussed as the Black Team is currently working on an altered version of their current designs that is adjusted for flight conditions. CFD is heavily used as these concepts will not be able to be truly tested without the use of a wind tunnel. The model tweaked for flight conditions will be presented as a CAD model with the CFD data but will not be printed. Mainly, this inlet concept is solely for the purpose of showing a slightly better model for actual flight. The reason for this design exploration is that the mass flow parameter analysis was completed only to design for a static test. Designing an inlet for simulated flight conditions is not necessarily within the deliverables, but still would prove useful to show the modifiability of the design when looking to integrate it within an actual aircraft. Since the main model, currently being iterated with a static test in mind, would not be designed for flight conditions- as it was not designed with these in mind- the thought arose that a second model could be adjusted from the first to include higher entrance speeds. CFD was used with higher speeds to create an inlet more viable for these conditions. This model is currently in a stage of

development that does not warrant an actual model, but CFD is currently being implemented for the development of this altered design.

Solidworks flow simulation was used to conduct CFD tests on the preliminary inlet designs. For the CFD analysis, certain boundary conditions and goals need to be defined. The first boundary condition will be placed at the inlet capture area. This boundary condition will be an environmental pressure of 14.696 psi, which is the pressure at standard sea level conditions. The second boundary condition is an outlet mass flow placed at the exit of the inlet leading into the engine compressor. The engine pulls in air at a rate of 0.512 pound mass per second, this will be the outlet mass flow boundary condition for the inlet. To find the average total pressure drop through the inlet certain goals will need to be defined to calculate the difference in pressure. The first goal was an average total pressure goal at the inlet face, the second goal was a total pressure goal at the exit of the inlet, and the final goal was an equation goal to calculate the difference between the inlet total pressure and the outlet total pressure. A depiction of the atmospheric conditions and the mass flow rate at the transition duct is shown in Figure 5.

As it pertains to the CFD model run on Solidworks, the boundary conditions were set to sea level standard day with a mass flow rate of 0.51 lbm/s at the engine, in accordance with JetCat specifications. Sea level standard conditions allows the team to correct parameters later to model the tests at any altitude and temperature. Global mesh settings were set to level 7, the finest possible. The was done to help gather data from the modeled probe faces, as they are extremely small, and to allow calculation for pressure recovery percentages. For the analysis settings, it was set to internal flow with adiabatic conditions. The working fluid is air, and the flow type is both laminar and turbulent, with no wall roughness. The finish settings had a refinement level of 5 for initial tests, but this was lowered to 3 for subsequent tests to help reduce the simulation run time, as the data difference between level 3 and level 5 refinements was essentially negligible. The analysis was set to complete once all predetermined goals were satisfied. These set goals were to calculate an average total pressure at the inlet mouth face, the upper and lower modeled kiel probes, and the outlet of the transition duct.

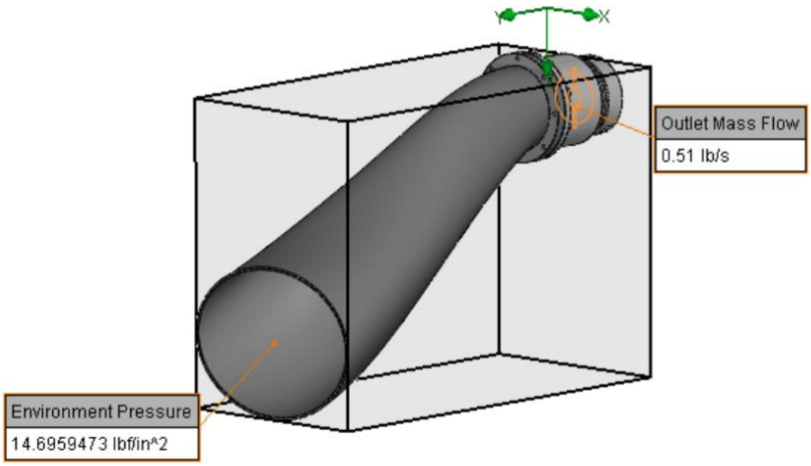

Figure 5: CFD Process Model

D. Finite Element Analysis

Before anything was mounted and constructed, FEA was undertaken to judge the safety of the plates mounting the engine to the thrust stand as well as FEA for the screws connecting the engine to the transition duct. Both were determined to be sufficiently safe for all foreseeable forces. All presented results from the team's analyses for the mounting plates, engine mounting ring, and the screws mounting the transition duct with a high estimate beyond what is expected.

The JetCat P100-RX model, shown in Figure 6, was used for the FEA. The transition duct attachment screws, placed equidistant from one another, is shown in Figure 7. FEA was conducted on the cowling screws that fasten in the transition duct as well as secure the inlet weight to the engine. In the most extreme case, which would entail some external force on the inlet causing such a force on the screws, fifteen pounds of force were distributed uniformly across the screws to simulate the downward resulting forces of the inlet and attachments on the screws, fixed into place by the engine. Even in this extreme case, the screws remained safe, a factor of safety over 1.0, and

most of the body of the screw exceeded 1.6 as its factor of safety. For this case, the max stress felt in the body was also well below, around 60%, of the yield stress. FEA confirmed the preconceived ideas that the inlet would be safe and perform well, but it also gave the team a sense of confidence that future designs would be able to be supported so long as they were within any reasonable build.

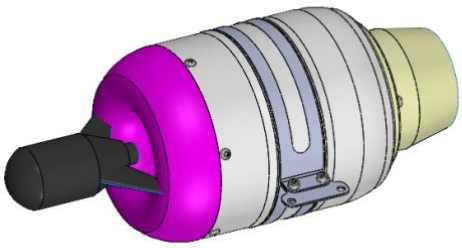

Figure 6: CAD Model of the JetCat P100-RX

Figure 7: CAD Model of Cowling with Screw Placement

Force Applied	15 lbf
Maximum Von Mises Stress	24656 psi
Yield Strength	41046 psi
Maximum Displacement	4.45e-5 in
Minimum Factor of Safety	1.23

Table 1: Finite Element Analysis Results

With the fifteen pounds of force modeled through FEA, which is far more than the team reasonably expects, there was not enough stress to yield the material, the displacement was a fraction of a millimeter, and the factor of safety was over one. With these being stated, the team was confident in their models not causing damage to the engine, the cowling screws, the test stand in case of critical failure, or the team member theirself. Less force than modeled is expected to be attributed to the inlets, and the moment arm apparatus is expected to carry some force, but the inlets would not cause failure even if this were not the case. The FEA provided confidence in the team's ability to move forward.

E. Passive Flow Control

Separation was seen as a big risk to the quality of the flow coming into the engine. There are two main ways to help this problem. The first is a longer, more gradual curved inlet. Since length is a secondary criteria, this was seen as a less than ideal solution. The next mitigation plan is for passive flow control to be used. Passive flow control is described to be structures that are built into the design to help the quality of flow such as bumps. The idea for implementation of this concept is keeping the inside skin of this inlet rougher in this area. Since most of the inside was sanded to ensure the flow would be going over a smoother surface, leaving this area rougher than other places may have a greater effect on the flow. This may allow for the flow to be tripped into turbulent and stay attached longer, much like the effect of dimples on a golf ball. However, the problem with this plan is the difficulty of implementation in a testing sense. Although the surface can be left rough, barring printing another inlet to completely smooth there is no way to truly test the effects of this roughness on the system. Although a good idea, the implementation means that an inlet will be completely wasted due to a tiny increase in performance over the other, differently sanded model.

An idea for more passive flow control is structures built into the design before printing. Structures, like dimples, could be built into the design that will be printed. These however, are not seen as feasible at the current stage of development. The inlet concept is currently being iterated to find an optimal overall design. Details within the design could be changed at a later time to include more of these passive flow control structures but this is not part of the inlet design at this moment.

F. Environmental Health and Safety Considerations

Some of the factors that would affect the design would include the environmental, health, and safety considerations, EHS. These considerations would serve to keep all members engaged with the project safe while also affecting team decisions about how to limit the social, economical, and environmental contentions. The team aimed to identify as many of these factors as possible, so that the design could be tested in a way to mitigate these into as much of a nonfactor as possible. While the team has a duty to AFRL to provide the best possible product, the team also has a duty to everyone affected by the project as a whole; balancing these responsibilities served as a guiding force in the design process.

The team identifies several safety procedures for themselves and for the safety of everyone near the test site. The team would stand a good distance away from the engine to stay clear from the exhaust gases and the extreme heat. Ear protection and eye protection must always be used when the engine is in operation. A fire extinguisher must always be available and on standby in case of a critical device failure to limit as much damage as possible to the team and to the equipment. Finally, the testing stand will have all structural loads tested to ensure that no structural failure is possible in any foreseeable fashion.

With respect to the COVID-19 pandemic, the team would have PPE (personal protective equipment) in use as well as following all the guidelines set in place by Oklahoma State University, such as the use of facemask when in a proximity of less than 6’ distance. Proper sanitation would also be used for the team and the test stand to keep health as a top priority.

Finally, the team identified environmental concerns that would be mitigated to keep the environment clean and minimize social impact. The team would only print parts that were necessary and run the engine once a week to keep it operating in peak condition but not test excessively to minimize pollutants from the fuel. The limited printing would lessen the waste and also free the printer for other teams or individuals who needed time to print for their project. Aiming for smaller build volumes also helps mitigate the material use consideration. Finally, the team has made sure to carefully store fuel, ensure all fuel lines are connected securely, and that any spills are carefully cleaned up with equipment designed for such a purpose.

G. Safety Guidelines

Beyond the social and environmental considerations that guided our design and shaped the processes by which the team conducted themselves and the project, the team was bound by the professional guidelines that outline all sorts of engineering considerations and safety concerns. From the National Archives and Records Administrations’ Aeronautics and Space guidelines: 14 C.F.R. § 33.75-33.78 (2021), the team identified the following sections of concern: safety analysis and engine ingestion. As it pertains to the safety analysis, the team took careful note of all safety guidelines governing engine mounting systems and the section on controls. For the engine ingestion concerns, the team identified and carefully observed the foreign object ingestion guidelines as well as the section detailing operation in rain and hail and the safety concerns those can dictate for engine ingestion. The Black Team also chose to consider the guidelines from the Occupational Safety and Health Administration (OSHA),

Section 1910. The guidelines covered encompassed PPE usage, proper sanitation, the use of a fire extinguisher, wiring design and protection, hazardous locations, and the storage of flammable liquids. Due to the scope of the project being the design and testing of a small engine, the degree to which careful adherence to safety guidelines was important but not critical. Failure on a project this small scale would not be thousands of dollars, severe injury, or a delay of more than a couple weeks. While important, the guidelines were not something that strongly geared the impact of the design beyond the obvious safety and cost measures. With all these considerations and guidelines in place, the team began work on designing the inlet.

Once these considerations were taken into account, other factors could be looked at. The main reason for other factors also being considered was the lack of resistance met when testing the CFD models. The pressure requirement, even with the added one percent buffer, had no trouble being met using the CFD model. Although it is not yet known how much of a discrepancy will be seen between reality and CFD, other factors were explored. These other factors revolved mainly around marketability. This is because the health and safety guidelines affecting the design were minimal in consequence. After both of these realizations were made, more creative inlet concepts were generated. This included more shapes being tested and a logo being to the side of the inlet itself. These more marketable, creative shapes allow for a more unique design than would be seen by others.

H. Risk Management

The APOP Black team considered a number of risks and created mitigation plans to decrease the severity of the consequences to an acceptable level. As can be seen below in Table 2, weighting was given to the severity of a consequence with the probability of the consequence occurring. Due to the scope of the project, a definition of the severity terms was included for context in the sense of the project. Catastrophic was defined as a two week or higher delay with a high possibility of danger. Critical was defined as a risk of a one to two-week delay with a risk of harm. Significant is defined as a delay between one day and one week with the potential for minor injury. Minor was defined as a delay of a day or less with no risk of injury.

		Severity of Consequence			
		Catastrophic (1)	Critical (2)	Significant (3)	Minor (4)
Probability	Frequently (A)	I	I	II	IV
	Likely (B)	I	II	III	IV
	Occaisional (C)	I	II	III	V
	Rarely (D)	II	III	IV	V

Table 2: Risk Management Table - APOP Black Team

Next, the specific potential risks were determined and a consensus was reached on how to rank these in order to then create a mitigation plan to limit the severity. For the determined risks, they can be found below with the corresponding level of risk (where higher numbers are more critical than lower numbers). Under each risk level are the corresponding risks pertaining to that level, the initial ranking of probability and severity (using the letter-number correspondence in the above table), the plan to mitigate the risk, and the level to which it has been mitigated. All these risks are shown below for reference.

Level I (Red):

- **Weather**
  - 1A, Level I, When conditions are unfavorable stay inside and aware, Mitigated to Level III (3A)
- **Exhaust Dangers**
  - 1B, Level I, 20 foot exclusion zone on either side of exhaust stream, Mitigated to Level III (3B)
- **Fire**
  - 1C, Level I, Outside testing with fire extinguisher nearby, Mitigated to Level III (3C)
- **COVID - 19**
  - 2A, Level I, Safety procedures outlined by Oklahoma State University, Mitigated to

Level III (3A)

Level II (Orange):

- **Test Stand Failure**
  - 1D, Level II, Over-designing mounting equipment and safe procedures, Mitigated to Level III (3D)
- **Hardware Hazards**
  - 2B, Level II, Safety procedures and trained peoples using equipment, Mitigated to Level III (3D)
- **Shock Hazards**
  - 2C, Level II, No exposed wires and safety procedures, Mitigated to Level III (3D)
- **Sound Hazards**
  - 3A, Level II, Ear protection and safe distance, Mitigated to Level IV (4A)

Level III (Yellow):

- **Fuel Danger**
  - 2D, Level III, Fuel is kept in outdoor shelter when not in use, Mitigated to Level IV (3D)
- **Test Stand Problems**
  - 3B, Level III, Properly securing testing equipment and storage indoors in designated room, Mitigated to Level V (4D)
- **Engine Ingestion Hazards**
  - 3C, Level III, Clearing test site of debris and testing in favorable weather, Mitigated to Level IV (3D)

Level IV (Green):

- **Material Waste**
  - 3D, Level IV, Frugality with material and fuel, Mitigated to Level V (4D)
- **Non-Design Testing Conditions**
  - 4A, Level IV, Using corrected parameters, Mitigated to Level V (4C)
- **Delays Related to Equipment Availability**
  - 4B, Level IV, Ordering equipment on time to prevent delays, Mitigated to Level V (4D)

Level V (Blue):

- **Storage Problems of Non-Harmful Material**
  - 4C, Level V, Test stand and engine secured indoors in dedicated room, Mitigated to Level V (non-problem)
- **Material Wear on Non-Critical Components**
  - 4D, Level V, Inspecting these components before use, Mitigated to Level V (non-problem)

I. Knowledge Gaps

There were some gaps in what was known going into the next phase of testing. The first of these is how well the CFD results fit with reality. This is a current unknown and must be tested as a part of the next phase of testing. Testing with the pressure equipment will be the main way to fill in this knowledge gap. Initially, there was uncertainty over how much of the axial length could be reduced while completing the requirements assigned by AFRL. This knowledge gap was overcome by extensive CFD testing, and models from eighteen to sixteen inches all performed well enough for different shapes and face areas to be used. Model interior changes are something to be considered, since the effects of friction and guiding structures (dimples, ridges, etc) have been unknown outside of

modeling. However, pressure testing using the kiel probes allows for better understanding and application for future iterations. Finally, the team was unsure about how to support the inlet and if the screws would be able to hold up the planned method. This knowledge gap has been filled by extensive FEA, and the constructed moment arm apparatus for the inlet worked correctly and supported the primary inlet; this is comforting since later inlet designs will be smaller.

IV. Experimental Arrangement and Procedures

The top view of the experimental setup shows the main structures associated with the current experiment plan. The engine as seen below is suspended within a circular mount attached to two mounting plates. Figure 8 shows the assembly fabricated to attach the transition duct to the inlet while relieving stress to the engine's cowling screws. This design is supported by the moment arm itself and not the surrounding safety cage or the table. No thrust loss will be expected from the arrangement due to the engine being rigidly attached to non-sensing elements. The plate conjoining the inlet and bell mouth transition piece was fabricated using wood as this material was cheap, strong enough to support the inlet, and easy to work with for the project.

Figure 8: Top View of the Experimental Arrangement

Figure 9 illustrates an aft view of the test setup, this further visualizes how the supporting structure for the inlet and transition duct is assembled. The faint red wire in the background of the picture is the lead for the load cell that measures thrust. The black, yellow, and red wire bundle is the control harness for the engine and finally the clear line is a fuel line feeding fuel mixed with turbine oil to the engine.

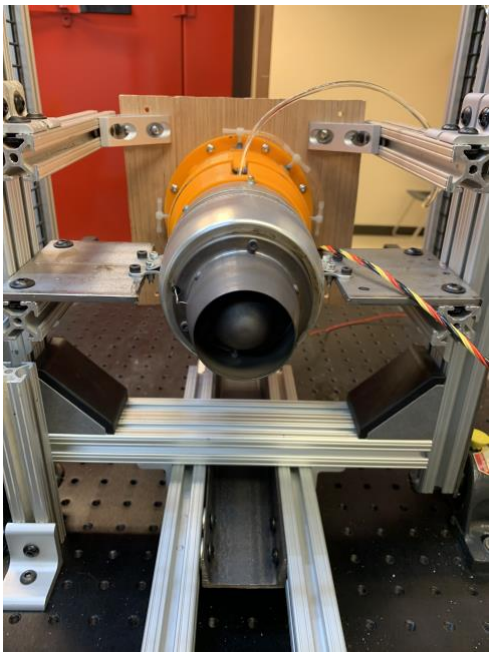

Figure 9: Back View of the Experimental Arrangement

Figure 10 is a profile picture of the test cell. Immediately aft of the wooden support plate are black spots with white and clear plastic tubing attached to them. These are static pressure ports, when coupled with a transducer these will measure static pressure while Kiel probes will be inserted at the 12 and 6 o'clock positions to measure total pressures. Having both static and total pressure measurements will allow the team to characterize inlet performance in terms of pressure recovery and predict performance in AFRL's test cell.

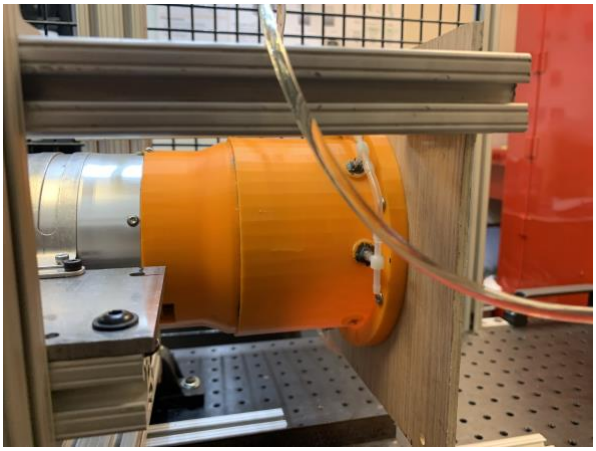

Figure 10: Side View of the Experimental Arrangement

Figure 11 is a front view of the test setup. This picture further details the inlet supporting structure. A black cylinder can be seen within the orange transition duct, this is the starter for the engine that the transition duct fits around. The transition duct is designed to replace the stock cowling of the engine while utilizing the stock cowling mounting screws. The silver circular pattern of screws is used to bolt the inlet to the support structure with the inlet having an identical flange and bolt pattern. When tightened the soft wood will act as a seal providing, ideally, and airtight seal. If needed this sealing can be augmented using solid or liquid gasket material.

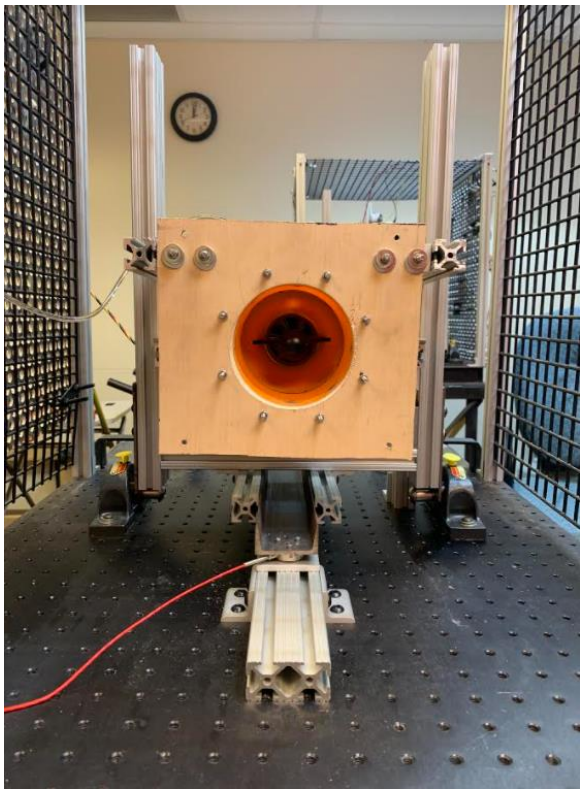

Figure 11: Front View of Experimental Arrangement Sans Inlet Design

The schematic for the engine test assembly can be seen below in Figure 12. This schematic details all of the major components used to operate and control the Jetcat P100-RX and the connections that are used in order to acquire the engine performance data such as RPM and TSFC. Additionally, the schematic for the pressure data acquisition assembly can be seen in Figure 13. In the assembly, two KAA-12 kiel probes are joined together through plastic tubing in order to find the average total pressure. This is then connected to a PX-409 absolute pressure transducer supplied by Omega. The static pressure ring is also connected to a PX-409 transducer. By knowing the static and total pressure, the dynamic pressure can then be found which indicates the velocity of the flow that is entering the engine. As it can be seen, these absolute pressure transducers convert the pressure inputs into a digital signal which is then directly imputed to a laptop. Through the use of the provided software, the pressure readings are then outputted.

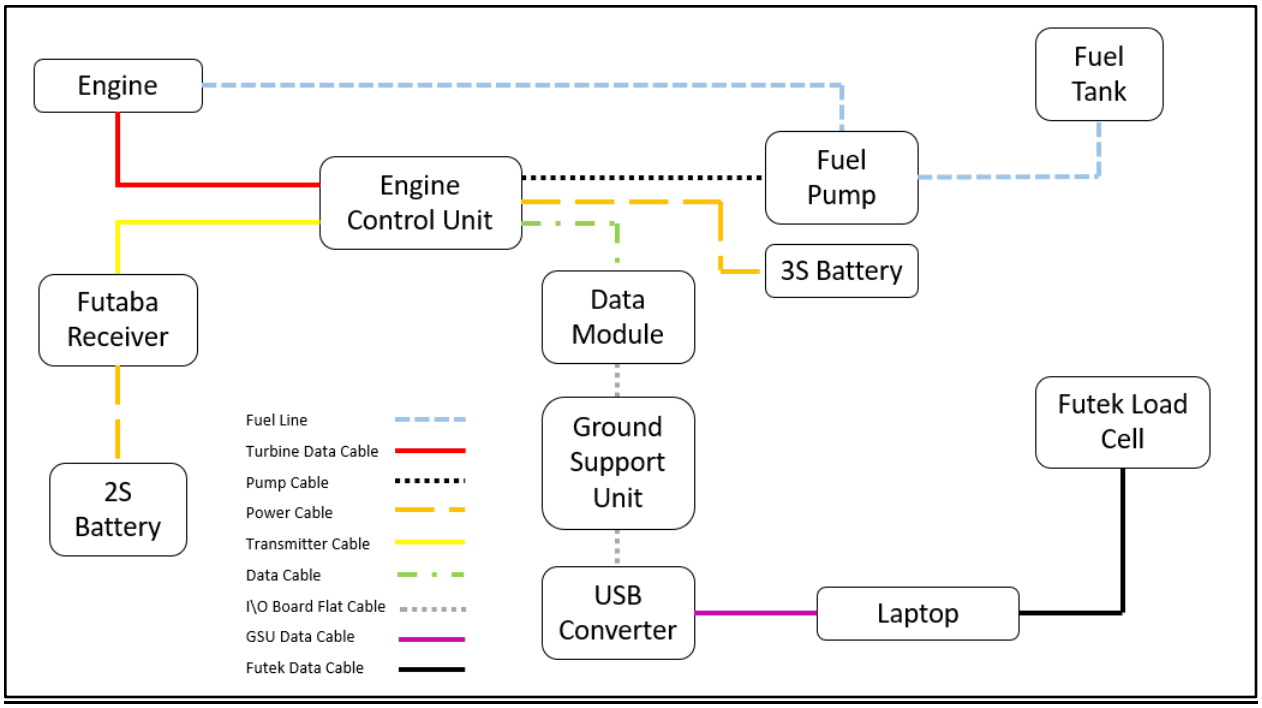

Figure 12: Engine Test Equipment Diagram

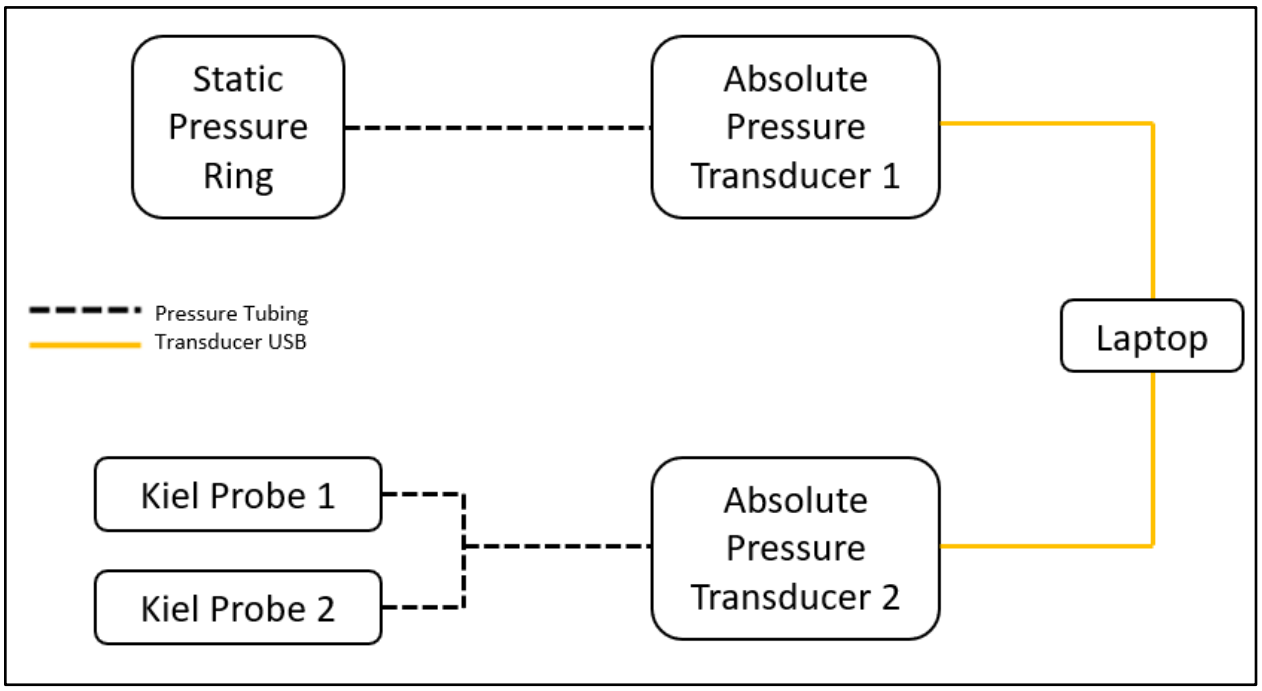

Figure 13: Engine Test Pressure Equipment Diagram

The testing procedure, based on the arrangement described above was then set forth so that data could be collected in a consistent and safe manner. The first of these procedures includes safety procedures that apply even when not testing. Every member of the team is required to wear PPE consistent with Oklahoma State University's COVID-19 protocols, even those that have been fully vaccinated. This is an important safety procedure that is

followed any time that the team meets and the same protocols are expected to be followed outside of specific meetings with the members of this group. In addition, all other safety procedures and risk mitigation plans, as outlined in the risk management, will be assumed to be followed during testing.

Testing itself will happen once a week to conserve fuel and prevent overuse of the engine. In addition, modifications have been made to the transition duct to ensure that the fit is optimal for the engine and can be used successfully. The main problem still experienced with this transition duct is that the duct must be removed to add the fuel line to the engine. This is due to the sharpness of the turn in the transition duct into the fuel line attachment point on the engine, in addition to the lack of space for the fuel line in the AFRL designed transition duct. In addition, holes were drilled into the second part of the transition duct to allow for the kiel probes and static pressure ring. These were planned changes and were placed in the locations marked by AFRL.

Steps to be taken before the test can be performed include checking parts of the stand to ensure nothing is loose or cracked. Correct placement is checked and screws are tightened to ensure safe operating conditions. The most at-risk portions of the test stand are checked before the test took place to ensure no damage would propagate during testing. In addition, the wheel locks are checked to make sure they will be able to be activated during the test. A fire extinguisher is brought outside in the event a fire takes place, a CO_2 fire extinguisher is specifically used. The cart is rolled out to the predetermined testing location with the laptops. The wheels are then locked and everything made sure to be secured.

During the actual testing, the fuel line is purged so the fuel is clean and coming straight from the tank. In addition, this acts as a way of making sure the fuel pump is working correctly. The transition duct is then removed so the fuel line can be placed into the engine. Everything is reattached and secured at this point. The kiel probes are placed into their locations and supported. The transducers are hooked up the kiel probes and the static pressure ring, if static pressure is sought after in the test. One laptop has the engine running software running and is recording thrust. The other is hooked up to the transducers to record the pressure measurements. The pressure recording software is briefly turned on to get an ambient pressure measurement before the test is run. Thrust measurements begin recording when the engine starts running so a full curve can be shown. OBS, Open Broadcast Software, is used to record the screen during the test so a live TSFC value can be recorded. This allows for a number of measurements over the entire rpm sweep. However, there was some technical difficulty in retrieving the OBS recording. Once this can be found, the TSFC values can be read over the rpm sweep. However, since no new tests can be performed, the one test that used this software will have to be used for this purpose.

The JetCat software is then used to start the engine. The first test includes, usually, the engine with the inlet. At this point, the engine is warmed up and the rpm is slowly raised to maximum in steps. Once the engine gets to about three quarters of maximum rpm, the pressure collection software starts recording. The thrust data is collected over the entire test. The engine is allowed to run at max rpm for about twenty seconds before being lowered slowly back to rest. The pressure recording is then stopped and the data exported to an Excel spreadsheet. The thrust data is also saved at this time. This happens during a cooling period of about three minutes to ensure nobody gets burned while switching the inlet. The reasoning for the engine with the inlet being run first is because the inlet can be taken off from the inlet side. In contrast, when putting the inlet on, someone has to be on the engine side holding the bolt. Doing it in this way ensures nobody is on the exhaust side of the engine soon after the test. Once the inlet is taken off, the process is repeated.

After the engine test, everything is saved and disconnected from the test stand. The transducers are taken off of the kiel probes and placed in a box on the cart. The fuel tank is removed from the fuel line and a specially purposed towel is used to absorb any spilled fuel. The batteries are also disconnected from the receiver and engine control. Once everything is disconnected and cleaned, the cart's wheels are unlocked and the cart is rolled back into the APOP room where it is stored.

V. Design Process

a) MFP

The design process began with basic calculations. Mass flow parameter was the main analysis completed during this phase of the project so the initial sizing of the inlet could be completed for the first round of designs.

These calculations were completed using Equation 2, as shown early in the report. The main extra assumption, besides the ones discussed, is an entrance velocity. This would be the velocity of the air going into the mouth of the inlet. Due to the nature of this project encompassing the creation of an inlet for a static test, the velocity assumed to be going into the mouth of the inlet was said to be fairly close to zero. In saying this, to avoid an extravagantly large mouth, the velocity was assumed to be about sixteen feet per second. Using the MFP equation, a mouth area of fifty-nine inches squared was determined to be the optimal mouth area. This optimal area was used until the first printed inlet could be pressure tested experimentally.

Mass flow parameter was also used frequently throughout the more detailed modelling later in the design process. The main purpose for these calculations was to size cross sections of the inlet to ensure Mach control. This allowed for better transition around curves, although the difference is fairly subtle. With the models taking advantage of this analysis, better pressure recovery could be achieved. Since the flow was to be sped up to reach the correct Mach Number to have a corresponding mass flow rate for the engine, the inlet nozzles throughout its length. This is an example of more rudimentary, qualitative analysis than was carried out but is a good example of the resulting shape, at least initially. Once the experimental results were found for the pressure, MFP became much less important as it was shown to be relatively inconsequential to the design.

b) Fanno Flow

Fanno flow was initially calculated to see the effects of boundary layer conditions on the pressure recovery. The drawbacks to using this as the estimation tool is that it is not of the same geometry as the inlet. This is because of the assumption that accompanies Fanno flow of a straight pipe. The analysis itself lends itself to finding a length to diameter ratio that would give a pressure value. However, this analysis was used to test the frictional losses of an already modelled inlet. The length of this inlet was measured from midpoint of the mouth to midpoint of the transition duct attachment. Using the cross sectional area at these points with the length, an average area can be found and converted into an average diameter for the straight pipe. After that, the length to diameter ratio can be used to find the pressure recovery. For the specific case of the first printed inlet, the Fanno flow estimates for the frictional losses ended up being about 0.23%. Although the Fanno flow estimates are very rough, the experimental results ended up matching well with them. This was relatively unexpected as the geometries were very different and very dependent on an assumed frictional factor. However, the closeness of the result obtained led to these being used throughout the design.

The results being very closed was mainly used in the estimation of the newer inlet later in the process, since this inlet could never be pressure tested. The results for this do not vary too much and are fairly dependent on the factors and assumptions discussed earlier. The main changes between the two printed inlets, to be discussed early, is the volume and the friction factor. The volume of the second inlet is much less than the first but the friction factor is also much lower. This lowering of the friction factor is attributed to painting and increased sanding on this iteration. This leads to relatively equal values for the pressure change with the decreased volume increasing the losses but the lowered friction factor decreasing the losses.

c) Initial Modeling / Design Selection

The team began their design selection by selecting shapes that they believed to be advantageous to the project requirements. Four inlet mouth shapes were chosen to best represent the range likely correlating to the best results. These chosen shapes were: Circle, Ellipse, Hexagon, and Octagon. A circle was seen as the simplest shape that is expected to have great results. An elliptical shape would allow for inlet turn angle modifications to be made much more easily, and the shape of the mouth could prove advantageous to the team's customization. A hexagonal shape was seen to be the simplest to manufacture and support, since the flat edges allow for easy clamping and printing, and the ridges could serve to guide the flow. Finally, the hexagonal shape was chosen as a compromise between the circle and the hexagon, since the shape is more complex, but it has the smallest model volume and has more ridges to guide the flow. These models were designed at 18" initially, since the team was not sure how much pressure would be lost to frictional effects, and starting at a length larger than needed would help the team determine

how much length could be reduced. The team also constructed a 12” model with each shape, and these results would later serve to conduct a sensitivity analysis correlating the length of the models with the estimated recovery.

Once this trend could be observed, the team could confidently pursue smaller models to get to a length that was deemed successful. Once that could be done, the team then would seek to limit the mouth volume and greatly shrink the inlet’s weight. Once an inlet could be printed, and the experimental losses could be determined, the team would then begin to iterate and create new models with results determining which inlets would be printed.

d) CFD Testing

Eight models were initially drafted to compare the effects of models with a different inlet shape as well as to determine the effect of axial length reduction. Once this data was collected, the team would then make a decision with which inlet mouth to use moving forward, and further axial lengths will be reduced pending the Sensitivity Study.

A frictionless test such as this will be missing a considerable amount of losses that will be attributed to frictional losses and other “real-world” losses that are not a part of this analysis. Most of these, such as heat transfer, are not very important so will not heavily factor into the pressure losses.

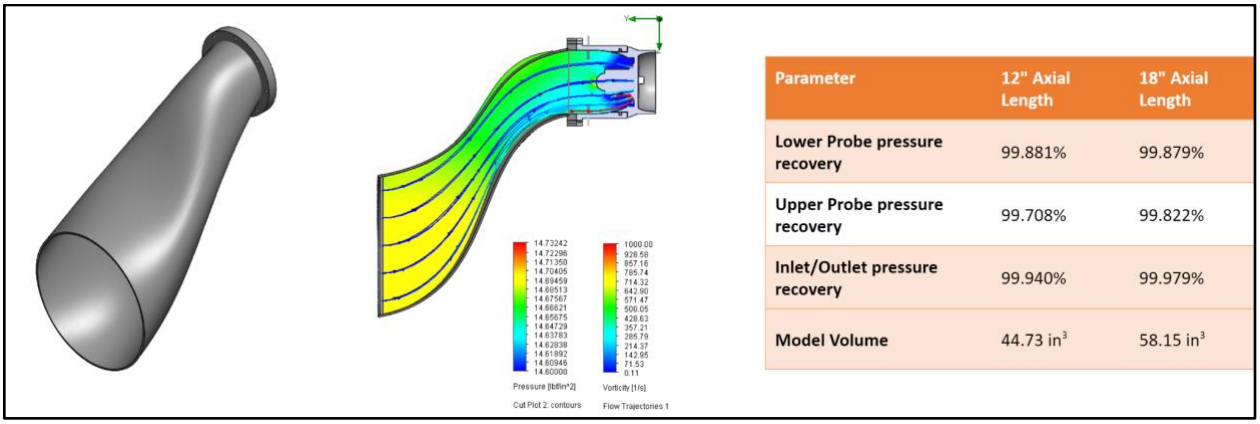

Parameter	12" Axial Length	18" Axial Length
Lower Probe pressure recovery	99.881%	99.879%
Upper Probe pressure recovery	99.708%	99.822%
Inlet/Outlet pressure recovery	99.940%	99.979%
Model Volume	44.73 in^3	58.15 in^3

Figure 14: 12” and 18” Circular Results

The results shown by the two circular inlets, thought to have the highest pressure recovery values, can be shown above. For consistency, the Inlet/Outlet pressure recovery will be used to compare between the concepts. This is more because the flow structure, as visualized above, lends itself to separation at the lower probe. The extent of this separation varies based on the axial length and volume of the inlet and gives more inconsistent measurements. The upper probe gives much more consistent values, up to three decimals on almost all of this batch of CFD testing. Although this shows that there is little change, it is almost a fault as there is no change at all between some models. The inlet/outlet recovery value shows much more expected values. In saying this, the values shown between the eighteen and twelve inch models have nearly negligible differences. The difference is about 0.04%, probably within the margin of error for the CFD tests. This allows

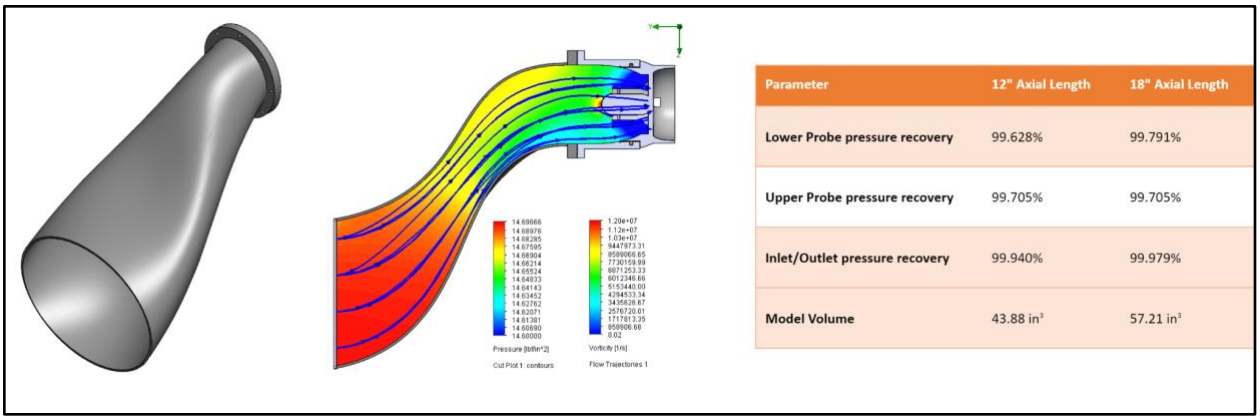

Parameter	12" Axial Length	18" Axial Length
Lower Probe pressure recovery	99.628%	99.791%
Upper Probe pressure recovery	99.705%	99.705%
Inlet/Outlet pressure recovery	99.940%	99.979%
Model Volume	43.88 in^3	57.21 in^3

Figure 15: 12" and 18" Elliptical Results

The results shown but the two elliptical inlets showed an overall pressure recovery nearly identical to that of the circular inlets, with the slightly lower recovery compensated with rounding. The elliptical inlets, however, showed these comparable results while also maintaining a smaller volume at each axial length than the circular inlets. The elliptical results showed worse recovery at each location, but negligently so and well within the margin of error.

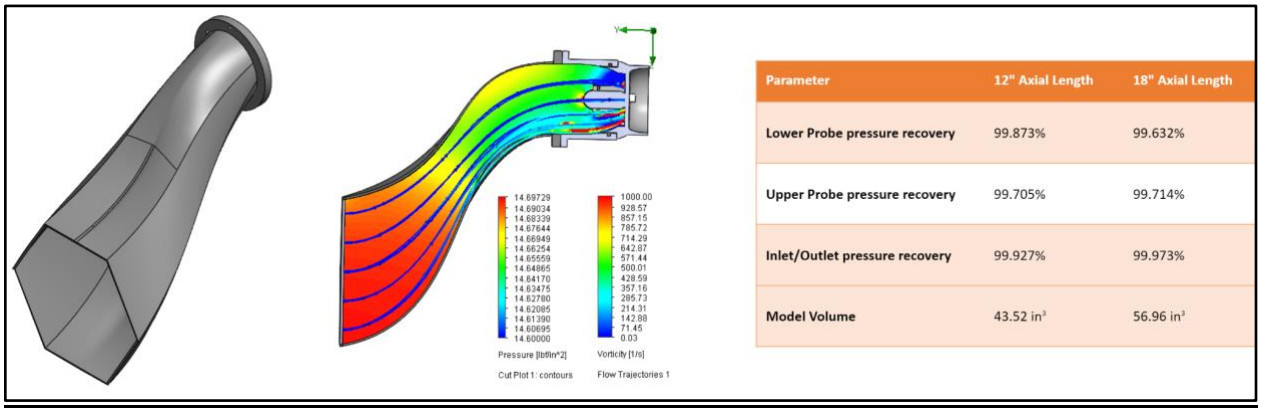

Parameter	12" Axial Length	18" Axial Length
Lower Probe pressure recovery	99.873%	99.632%
Upper Probe pressure recovery	99.705%	99.714%
Inlet/Outlet pressure recovery	99.927%	99.973%
Model Volume	43.52 in^3	56.96 in^3

Figure 16: 12" and 18" Hexagonal Results

The hexagonal inlets are by far the most unique. The shape stands out, and is sure to draw attention, though maybe not for the right reasons. The hexagonal models had shorter model volume than both the circular and elliptical models shown above. The recovery, however, showed the lowest value of any tested shapes at the same axial lengths. The team attributed this to too much space between the ridges, causing the intended flow guidance to result in flow bunching up instead. It performed close enough to the other models when at 18", but it had a higher drop at 12" than either of the previous models, and the shape did not lend itself to shortening beyond 9", which the team later surpassed with different models.

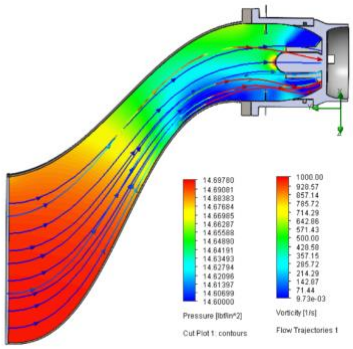

Parameter	12" Axial Length	18" Axial Length
Lower Probe pressure recovery	99.650%	99.895%
Upper Probe pressure recovery	99.856%	99.767%
Inlet/Outlet pressure recovery	99.928%	99.976%
Model Volume	43.17 in^3	56.48in^3

Figure 17: 12" and 18" Octagonal Results

The octagonal inlets showed slightly better recovery than the hexagonal model when at 12" and below, and the shape lended itself to shortening models down to even around 6". The octagonal models boasted the lowest inlet volume of any model made for each axial length, and the recovery was less than the circular and elliptical models, but greater than the hexagonal model. The recovery at the upper probe was the highest for any 12" model, and the lower probe recovery was a decent middle ground. The octagonal model seemed like a great compromise between promising recovery values for the smallest print volume.

e) Graphical Performance Comparison

Following the accumulation of all initial data, the team constructed a Graphical Performance Comparison to help aid visualization. All tests run listed above are shown in the Figure 18 below, comparing the upper and lower probe recovery values as well as the recovery value experienced throughout the inlet as a whole.

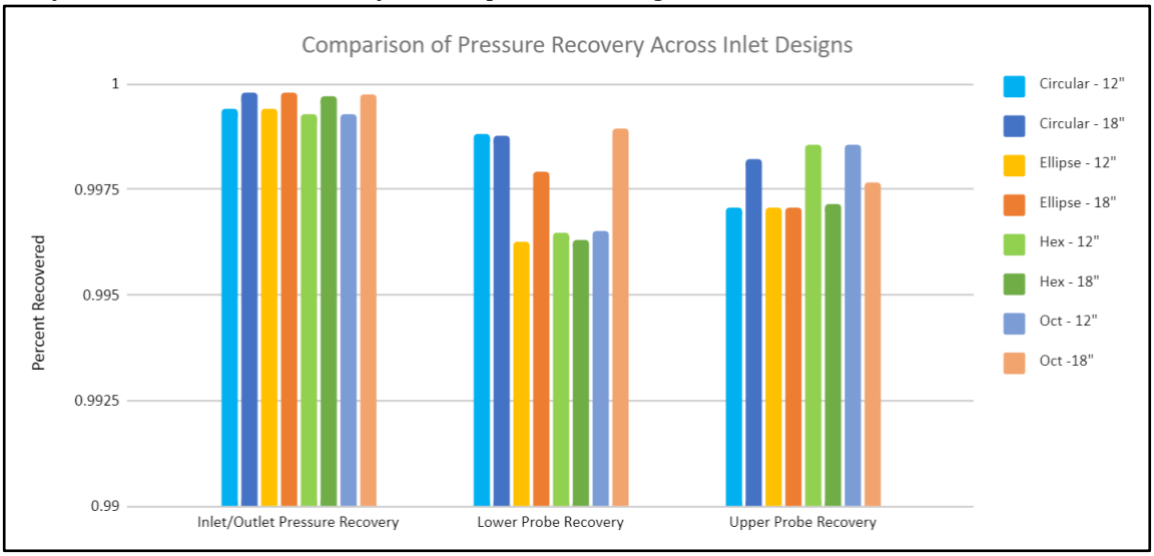

Figure 18: Graphical Performance Comparison

As can be seen from this graph, the change in axial length affected the results more than the change in mouth shape, as it relates to total pressure recovery. Even with the axial length difference, all recovery values are effectively the same, with the difference being less than a tenth of a percent from the worst performing initial inlet to the highest performing initial inlet. The results were promising for all concepts, and now the team had to evaluate these factors as well as weigh the primary and secondary project criteria to select which inlet shape to use moving forward.

f) Weighted Decision Matrix

To aid in the selection of the ideal inlet to begin iteration on, the team constructed Figure 19, the weighted decision matrix shown below. The team chose to weight the values of Length, Turn Index, Cost, Volume, Pressure Loss, Visual Appeal (which factored in manufacturability and marketability), and the Complexity of Build.

			Design Concept					
*Mouth Shape (Axial Length)		Weight	Circle (12")	Circle (18")	Ellipse (12")	Ellipse (18")	Octagonal (12")	Octagonal (18")
Criteria	Length	0.2	0.15 (12")	0.1 (18")	0.15 (12")	0.1 (18")	0.15 (12")	0.1 (18")
	Turn Index	0.15	0.1	0.15	0.1	0.15	0.1	0.15
	Cost	0.1	0.1	0.1	0.1	0.1	0.1	0.1
	Volume	0.2	0.15 (44.73 in^3)	0.1 (58.15 in^3)	0.15 (43.88 in^3)	0.1 (57.21 in^3)	0.15 (43.17 in^3)	0.1 (56.48 in^3)
	Pressure Loss	0.25	0.25 (99.940%)	0.25 (99.979%)	0.25 (99.940%)	0.25 (99.979%)	0.25 (99.928%)	0.25 (99.976%)
	Visual Appeal	0.05	0.025	0.025	0.01	0.01	0.05	0.05
	Complexity of Build	0.05	0.05	0.05	0.05	0.05	0.05	0.05
Results			**0.825**	**0.775**	**0.81**	**0.76**	**0.85**	**0.80**

Figure 19: Weighted Decision Matrix

The matrix was constructed initially to help ease the selection process and decide which inlet mouth shape was declared the winner and would be further iterated on. As easily noticed above, though the longer 18" models have better performance, the increased cost, time to print, length, and volume held each 18" inlet at a lesser weighted score than the respective 12" model for the same mouth shape. Another thing to note is that the hexagonal model has been entirely eliminated at this point, as it held no benefits over the octagonal model; it looked less appealing, performed worse, and had a higher model volume. All pressure values were so similar - within a tenth of a percent - that the team felt weighting them substantially would be something not worth the score. This difference could easily be attributed to uncertainty, error, or some other factor and is not entirely indicative of a better inlet. To the same end, the volume of the octagonal model was the smallest of any of the options, but that decrease in volume, though more substantial than the loss in pressure, was still seen as a value so small, that a difference in the scoring need not apply.

The team still had to choose an option, so that is where the differentiating factor of the visual appeal was weighted. When choosing this score, the team had to weigh their personal opinions on how easy the inlet would be to manufacture, support if needed, as well as how well the design could be marketed, based on performance and how good the inlet looked purely on its visual merit. The team conducted anonymous voting, and it was decided that the octagonal inlet best encompassed all these values in a vote of 5 - 1, with the circular model being placed second and the elliptical model being placed third. With the team's majority opinion, the lowest model volume, and comparable results, the team decided on an octagonal inlet mouth for the foreseeable future tests.

g) Sensitivity Study

After obtaining the data from the eight initial models, the team plotted the recovery percentage compared with the model volume to determine a trend and see how much the model could be reduced. The peaks are attributed to the elliptical models due to their comparable recovery with lower volume, and the valleys are attributed to the hexagonal models with their poorer recovery.

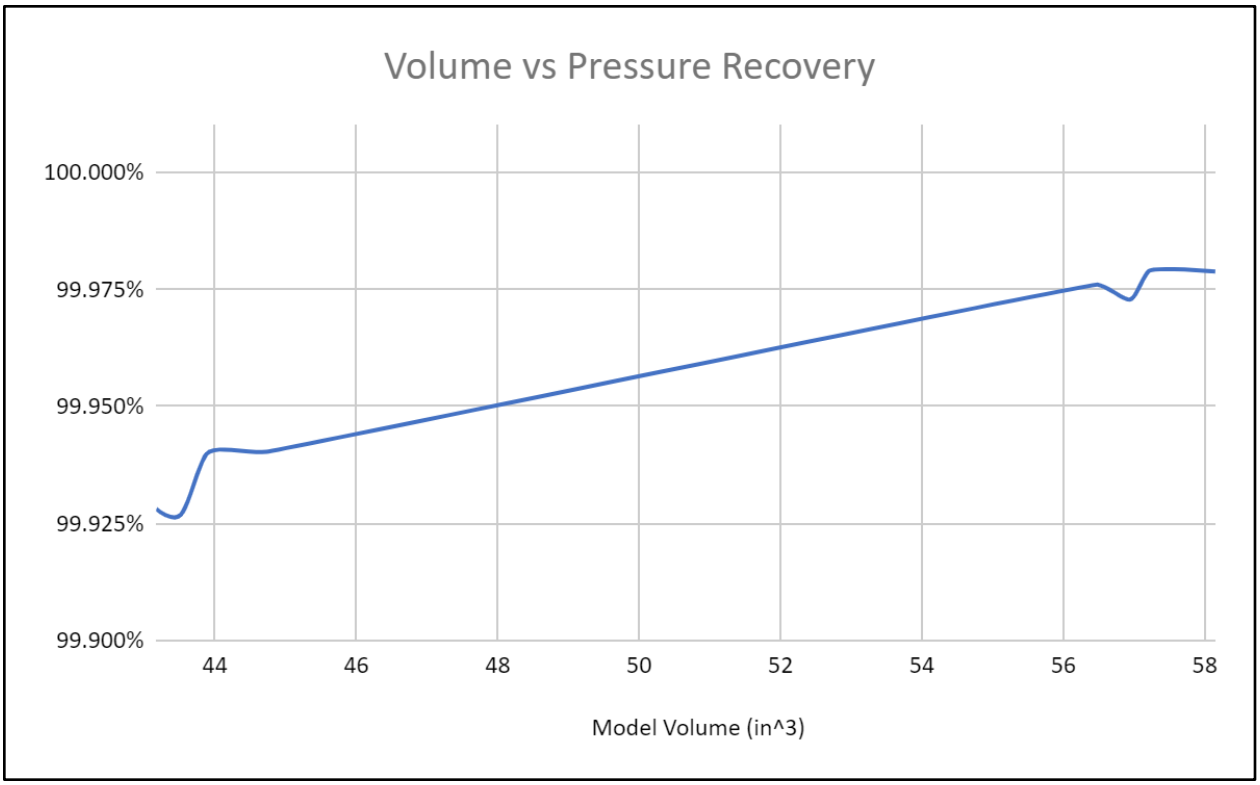

Figure 20: Sensitivity Study

The trend shows that a decrease of 14 cubic inches only resulted in a recovery change around 0.05%. This information showed the team that decreasing the axial length to both 9" and 6" should, theoretically, keep the recovery percentage well over what is required by the project specifications.

h) Model Reduction

With the sensitivity study trend showing that a decrease in volume caused by a reduction in axial length gave promising results when it came to pressure recovery, the team decided to test both a 9" model and a 6" model to see how small the inlet could reasonably be. At this point in the project, the team did not foresee use of anything less than 6" in axial length and chose to decrease the inlet mouth area moving forward. The team reasoned that reducing the axial length below 6" while not addressing the large volume created by the large mouth was a less important issue. Decreasing the surface area of the inlet would be the next way to decrease model volume while maintaining an inlet at reasonable size.

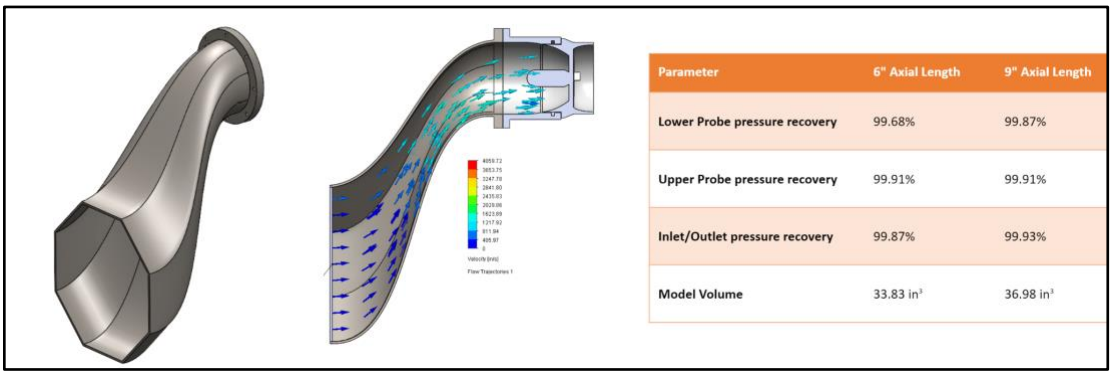

Parameter	6" Axial Length	9" Axial Length
Lower Probe pressure recovery	99.68%	99.87%
Upper Probe pressure recovery	99.91%	99.91%
Inlet/Outlet pressure recovery	99.87%	99.93%
Model Volume	33.83 in^3	36.98 in^3

Figure 21: 6” and 9” Octagonal Results

As it pertains to the results of the 9” and 6” tests, the 9” still showed a pressure recovery over 99.9% at a model volume slightly under 37 cubic inches. The 6” model was able to decrease the model volume of the inlet by over 3 cubic inches, but the overall recovery dropped to 99.87%, the first model with a recovery below 99.9%. While this recovery is still more than acceptable given the team’s criteria of ensuring a recovery value above 98%, the team chose to keep the 6” model as it was to determine the losses due to friction before further iteration would be made.

VI. First Iteration

With the idealized recovery results of 99.87%, the team chose to take the 6” inlet, as it was sized by MFP and showed a recovery more than needed. The team was not sure what kind of frictional loss to expect after printing and sanding the inlet, so this model was chosen because it was at a good axial length and would still perform if 1.5% was lost overall. The 6” octagonal inlet was printed in three parts, one part for the mouth, and two parts for the flange and the top half of the inlet. The inlet had the PLA support removed and sanded down to result in the smoothest inlet possible, and JB Weld was used to adhere the inlet together, and all interior JB Weld was removed with a dremel and sanded to keep the interior smooth. The complete, first iteration print can be seen below in Figure 22.

Figure 22: 6” Octagonal Inlet (Iteration 1)

Below, this inlet is shown fastened to the transition duct on the test stand. As the picture was taken, data was being collected for the inlet to see how it performed in terms of pressure recovery and thrust loss, as well as

determining how much was lost to friction. Once this could be determined, further iterations would be attempted with an expected frictional loss being about constant.

Figure 23: First Inlet Iteration - Testing

VII. Experimental Results

CFD was conducted on a variety of inlets, and after the team observed the results and took a vote for which inlet shape was the best compromise of primary and secondary grading criteria, the octagon was selected. Once that was determined, the team conducted analyses on inlets from eighteen inches to six inches. The values for all the Octagonal inlets are tabulated below in Figure 24. The percent of total pressure recovery is shown on the y-axis and the location for the recovery data is shown on the x-axis.

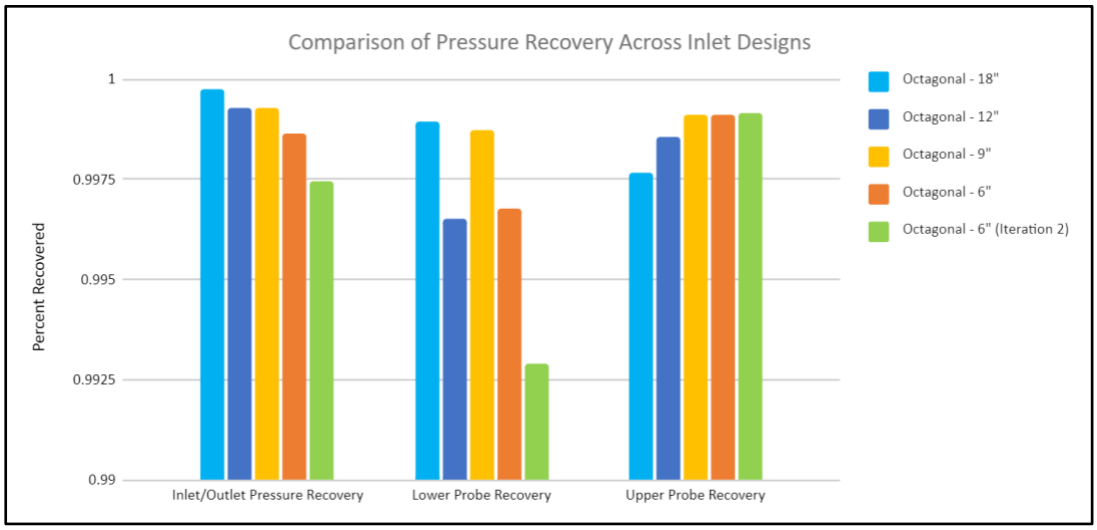

Figure 24: CFD Results for Relevant Design Concepts

As can be seen by the chart above, there is very little variation between the pressure recoveries of all of the octagonal models tested. All of the models are within a 0.01% of each other. This is especially key with the smallest inlet concept seen to be very close in pressure recovery to the other values, meaning that it is a viable option. The main importance behind this is that this inlet could not be tested due to engine problems. The CFD results, however, are shown to be very close to the experimental values in the one concept that could be tested, the octagonal six inch model with the largest mouth.

There were several data sets collected during the course of testing the inlet design. To this point, there were two main layouts tested with the datasets being named for these differences. The first set is without the inlet bolted onto the transition duct. The second layout has the inlet cantilevered off of the transition duct. Tests were conducted weekly, and once the pressure measurement apparatus was installed and the transistors' software ready to write data, the team tested and rendered these results for thrust and pressure.

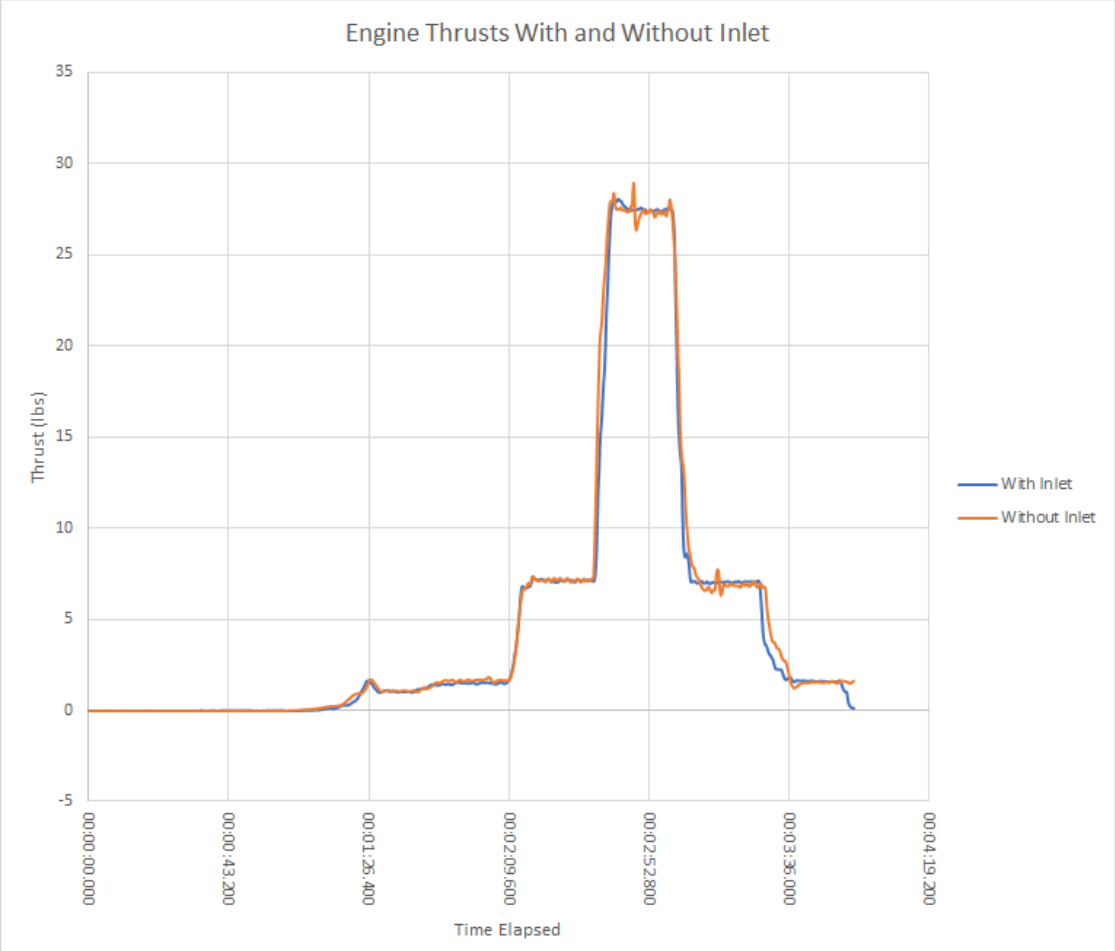

Figure 25: Thrust Results - April 1st

With the thrust test being conducted simultaneously with the pressure test and calibrated summarily, the team was confident in seeing that the initial testing with the first inlet, sized ideally through MFP, performed as expected and kept the thrust loss consistent with earlier testing. As can be seen from the chart above, the thrust loss is essentially negligible with the inlet attached or detached. There is some slight thrust loss but, as expected, the thrust will not encounter meaningful enough losses to be the driving factor for the design; the pressure loss will be the critical factor determining just how much further iteration can be achieved. This can be seen by both the engine with and without the inlet recording thrust estimates around twenty-four pounds. There is a very slight decrease in the thrust seen by the engine with the inlet, as expected, but this decrease is nowhere near the five percent loss maximum.

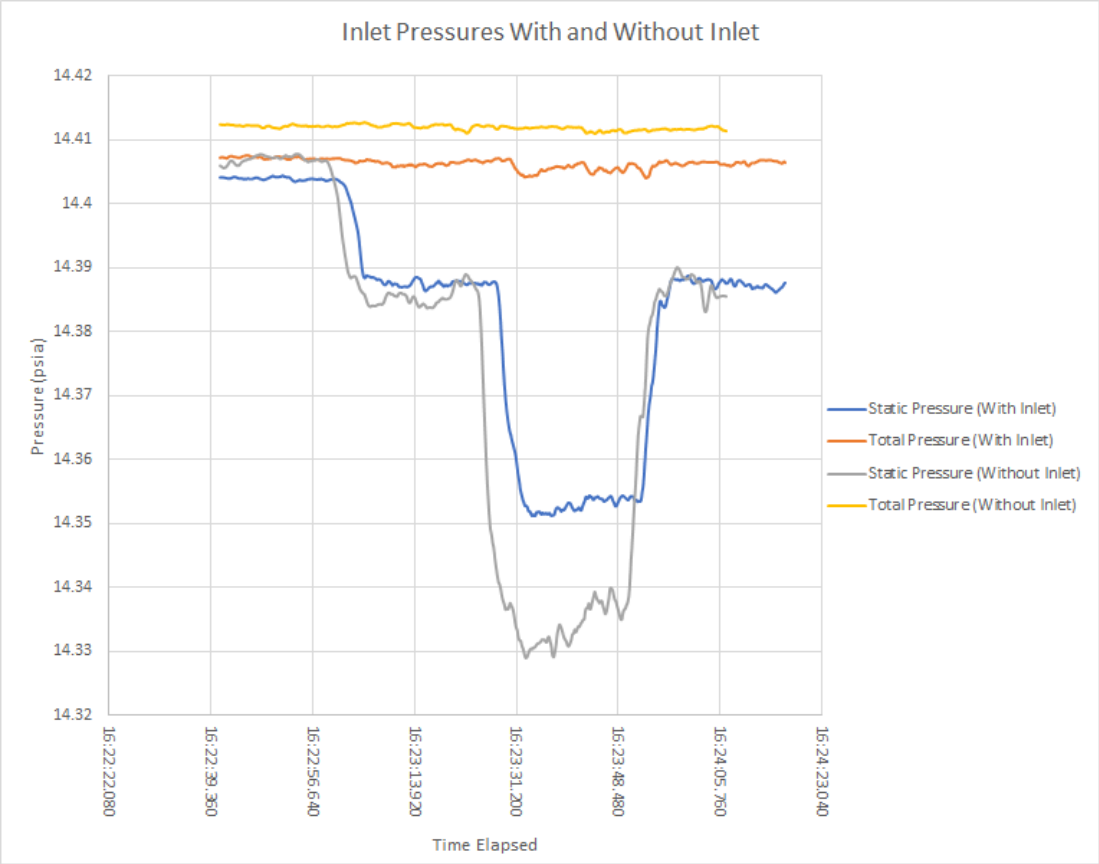

Figure 26: Static and Total Pressure Composite Results - April 1st

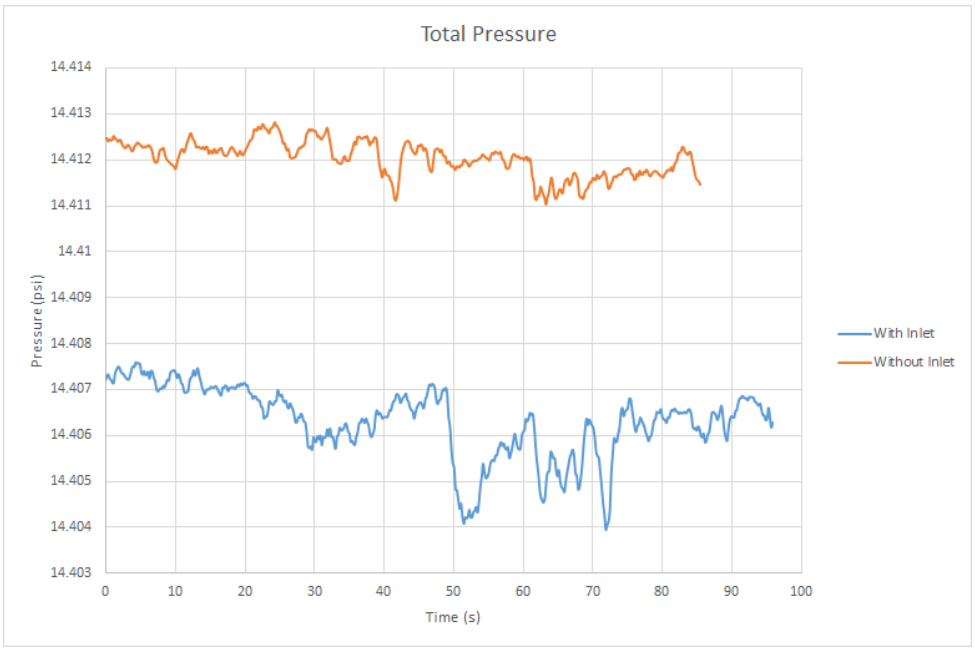

Figure 27: Total Pressure Results - April 1st

The team's first pressure test instilled a great amount of confidence in future iterations allowing for significant drops in volume. Though the MFP sizing was ideal to speed up the flow to the desired speed for the

JetCat to operate ideally, the team was more than surprised to see the frictional component only resulted in a total pressure recovery of 99.57% when compared to a test without the inlet. The MFP was sized with a normal, non-windy day in mind, but given the outdoor conditions being slightly windy, paired with an inlet size designed to funnel static air to the desired flow rate naturally, led to an incredible recovery. The first inlet was only sanded and was not primed or painted to smooth over the internal structure any more than just sanding; the team believes that these methods would have further increased recovery by decreasing friction and roughness. The shorter axial length does not allow for friction to be too much of a concern, but the team will further explore the results from decreasing mouth area and possibly increasing axial length. The results were more promising than expected, and the second iteration will be shown below detailing the changes made and how the further iterations affected the results.

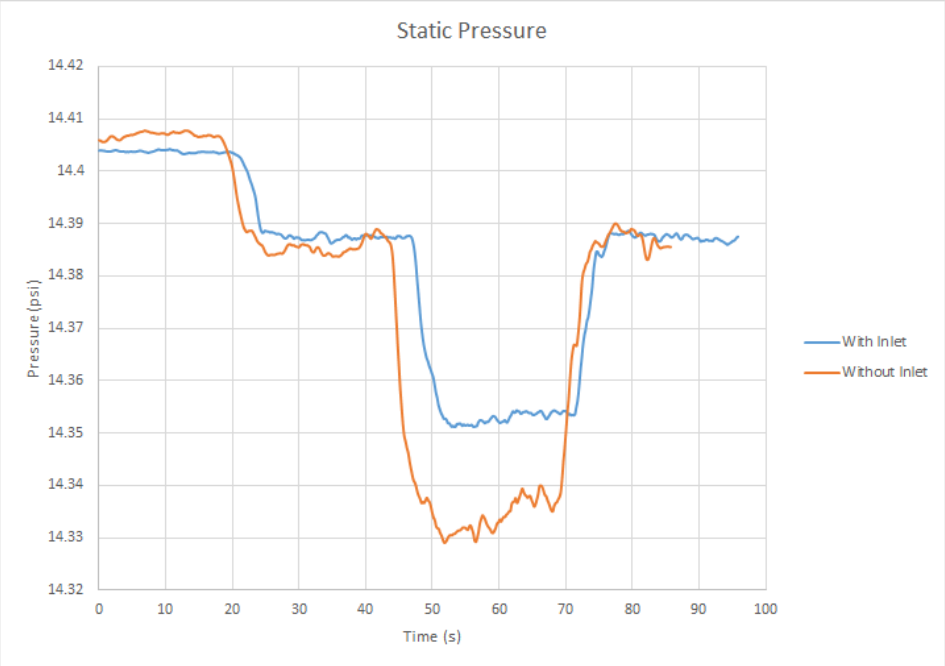

Figure 28: Static Pressure Results - April 1st

The team's readings for static pressure showed more deviation than either the total pressure or the thrust component when compared to tests with and without the team's custom inlet. The losses seem to be about three times the losses when compared to the total pressure losses, but given that the static pressure tests serve to help judge velocities. It is not a scoring criteria, but it helps keep the team informed about changes and concerns that may affect the total pressure later on. Static pressure is mainly used in conjunction with the total pressure as a way of showing how much of that total can be attributed to the dynamic pressure. Since dynamic pressure is mainly affected by the velocity of the air, it can be used to find the velocity of the air coming through the transition duct.

The other important variable tested for during this experiment was the specific fuel consumption, or SFC. The SFC is a criteria commonly used to determine the effectiveness of the inlet at keeping the flow "clean". In addition, AFRL is using SFC as a testing criteria, with the maximum SFC increase being five percent. The testing method for this measurement was debated, however. This was because the JetCat software actually gives a live value of SFC that can be read. By using a screen recording software, this can be saved for plotting of key points in the rpm sweep, as can be seen in figure below.

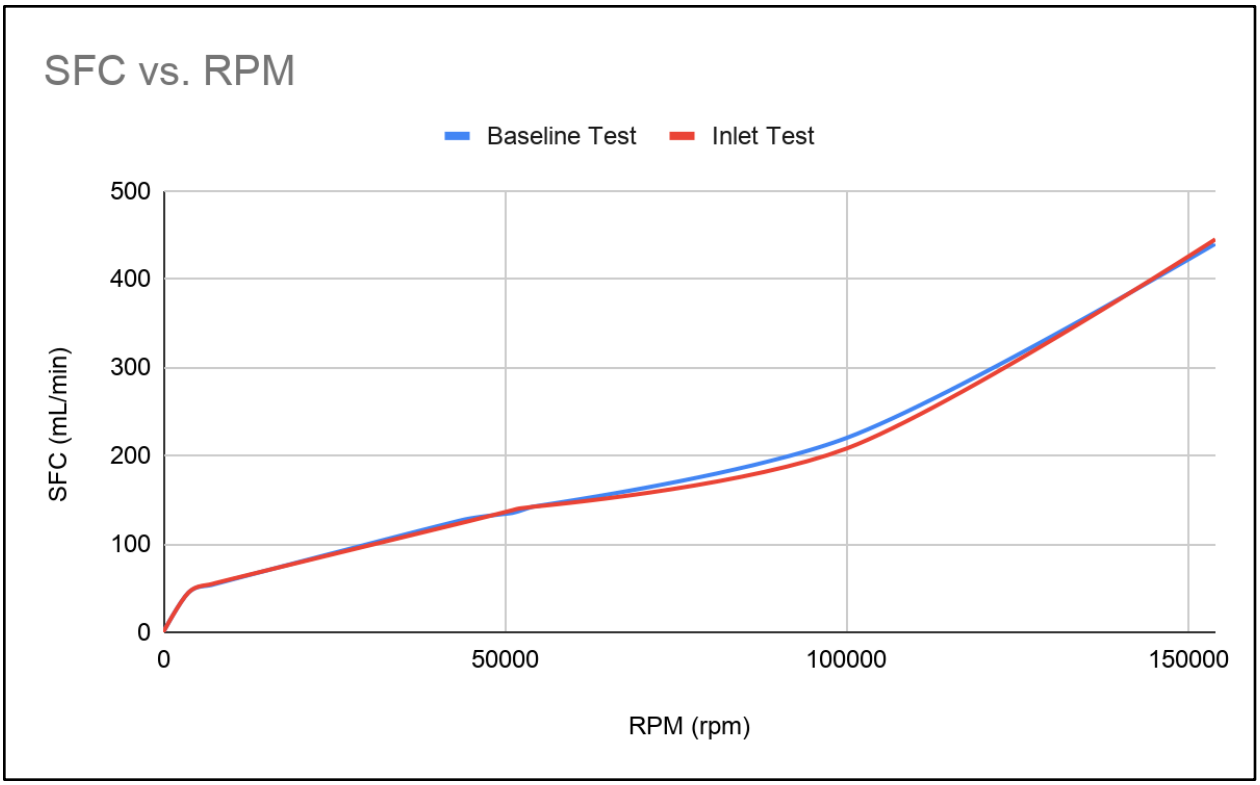

Figure 29: SFC Measurements Over RPM Sweep as Read from JetCat Software

The drawback of this data comes in that the measurement is very inconsistent and seems to be inaccurate. The reasoning behind this being the belief is that the data is very dependent on how long the engine is allowed to idle at a certain rpm. In addition, it can be seen at many points on this graph that the SFC is higher on the test without the inlet than with the inlet. The values are similar enough that it is believed to be within the uncertainty of the measurement, although slight variations in conditions could also affect the value in these minor ways. However, going off of these values leads to an assumption that SFC will not be much of a problem. At the maximum rpm condition, the SFC growth from without the inlet to with the inlet is about one percent. The SFC has a clear relationship with the rpm, with exponential-type growth as the rpm increases to full throttle. The values taken were fairly rough as more averaging could have been done, as opposed to the current method of taking a few points near each rpm reading.

The JetCat software data, however, is seen as inaccurate to the real values. The values are very inconsistent and vary during the actual test. A much better system of measuring this variable was considered for later tests but was unable to be implemented due to the engine failure. This method includes using an accurate measuring scale to test the weight of the fuel tank, with and without fuel, at the beginning of the test and at regular intervals throughout the testing. This would be much more accurate if done properly. However, because only one test was able to be done with the screen recording software, this plan was not able to be implemented. The data from the JetCat makes sense in trend but it is not very intuitive that the test with the inlet would be more efficient than the baseline test. This is due to quality of the flow being decreased in this case, although fairly minimal were seen with this iteration. It is unlikely that, although the values probably differ from reality slightly, the SFC would be in any danger of eclipsing the five percent threshold. Most of the points taken for the SFC plot lead to a maximum percent difference of about one percent. There are greater differences in other parts of the chart, with the one percent growth seen at maximum rpm, that show an almost six percent decrease in SFC when the inlet is installed compared to the baseline. This shows some inaccuracy in the data.

The CFD can also be compared to these results. The pressure values of the engine with the inlet and without the inlet were used to find the percent recovery of the system. This was then compared to the value shown in the CFD. The differential between experimental and theoretical values can be estimated with this. The values were expected to be different because the CFD did not have a frictional component. This was the main contributing factor to the difference. The pressure recovery value seen, as a percentage of the inlet-less engine, was found to be 99.57%. This can be directly compared to the value of about 99.8% calculated by the CFD. Therefore an assumption can be drawn that the difference is small enough between the theoretical and experimental that a much smaller inlet would be viable. The thrust values also showed a very small difference between the baseline tests and the test with the inlet. The pressure is now seen as the limiting factor of the size of the inlet, although there is also a very small decrease in the pressure recovery.

After design decisions were made based on the results shown above, an inlet with a much smaller build volume was created. This inlet took advantage of the clear buffer that was seen after the pressure results could be found. The inlet build volume was cut in half during this design process as it was seen as a viable choice after the CFD phase of the design. The experimental results of the slightly larger inlet concept show that this could be a possibility. This concept was built and sanded to be ready for testing. However, due to technical issues associated with the engine or testing equipment, this concept could not be tested experimentally.

VIII. Second Iteration

After the success of the six inch iteration, another analysis was run with the same six inch octagonal inlet but with an inlet surface area more than halved from what it was determined to be through MFP. Figure 30 shows the total pressure distribution found in the CFD tests for the small-mouth, 6-inch inlet. This was the team's most recent print, but it has not been tested as Phase II deliverables were cancelled due to Covid-19 complications. The team believes that this inlet would have been close to the final inlet, needing one or two more slight revisions if testing were to be done. The results for this inlet are shown below compared to all the other inlets run so far. While it does have the lowest recovery values so far, it still has a near 99.75% estimated recovery.

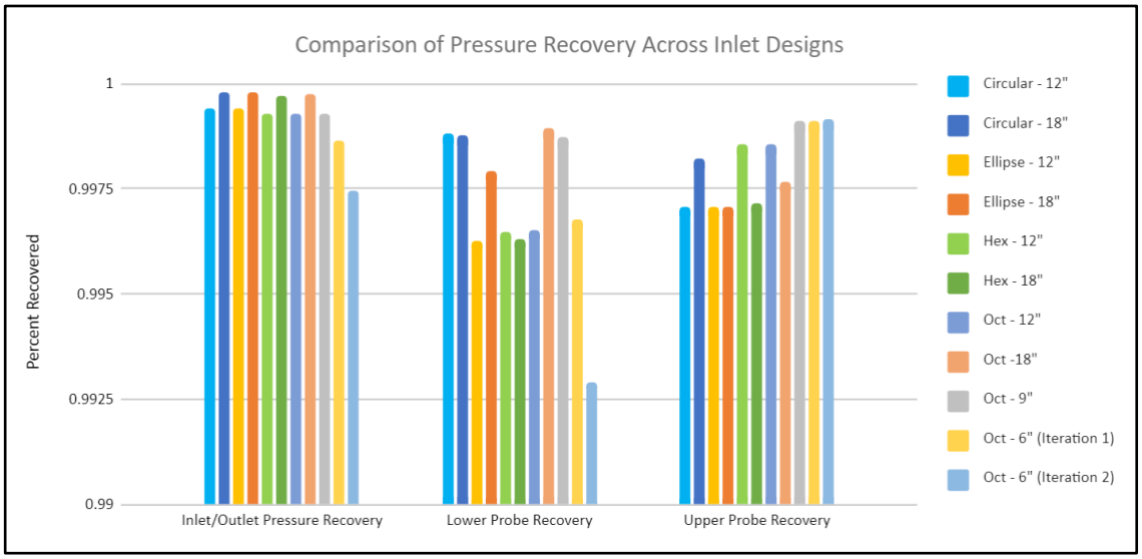

Figure 30: Graphical Performance Comparison (Through Iteration 2)

Figure 31: 6” Octagonal Inlet (Iteration 2)

The inlet can be seen above in Figure 31 after sanding, priming, painting, and clear coating. It can also be seen next to the previous inlet in Figure 32 below to compare the drastic difference between the two. The drop in pressure due to the reduction of the mouth area seems to correlate to a difference of around 0.013% from the above graph. However, this decrease in pressure also dropped the total 3D printing time from 106 hours to around 36 hours. The decrease in volume was significant, and the need for support was greatly decreased.

Figure 32: 6” Octagonal Inlet (Iteration 1) Side-by-Side with 6” Octagonal Inlet (Iteration 2)

Figure 33 below is beneficial in visualizing the flow as it goes through the inlet. Using this, it can be seen that the main areas of concern are right after each curve. Passive flow control could be used to help negate some of these effects. However, these areas will only become worse as the axial length lessens. These results are useful only in showing areas of concern as the results themselves will vary with reality. The pattern shown by the CFD will

presumably stay relatively constant throughout the iterations. The areas around the curves are of great concern as these “cooler” colors show lower pressure values. These are the areas where the flow will separate from the surface. Extra care can be taken in these locations to help the flow either stay attached longer or reattach sooner.

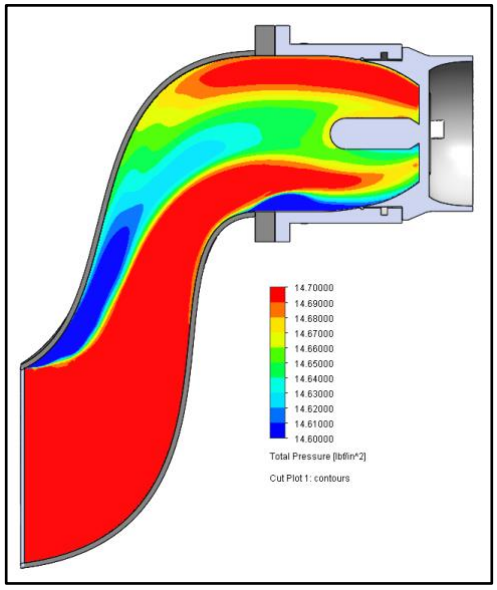

Figure 33: CFD Visualization (Static) - Octagonal 6” (Iteration 2)

With the experimentally determined 0.25% drop in pressure from the CFD results to the engine test for the first iteration, the team decided to work with no less than an expected 0.30% drop for all models to ensure that an iteration does not step too far and exceed the project requirements. With the expected drop of 0.30%, the team expects that this second, smaller iteration will succeed and still leave room for further improvement with respect to the axial length and the mouth size. As can be seen in the graphical comparison of Figure 14, the small inlet still shows an expected recovery of over 99%, though the experiential recovery will be closer to 98.75% after factoring in the estimated additional loss of 0.30%. Due to the closure of the Project before Phase II and the decrease in funding, the team could not pursue a test to verify these results.

IX. Flight Conditions

CFD tests were run to test the current inlet iteration at simulated flight conditions, beginning with a flight speed of Mach 0.5. The figure below shows the total pressure distribution in the inlet using the flight conditions. A table showing the goal results of the simulation has also been included. While this inlet had an average performance outside of the AFRL testing standards, the pressure drop seen by the probes is lower than what may have been expected for this increase in speed. The main areas of concern with this current inlet design, should it be implemented at this flight condition, would be flow separation at the turns. This can be seen in the pressure plot, as the areas with the greatest drop occur immediately following a turn. This may be mitigated by using different spline angles or extending the axial length of the inlet. In addition, passive flow control methods such as slightly rougher skin or dimples could be implemented and tested later.

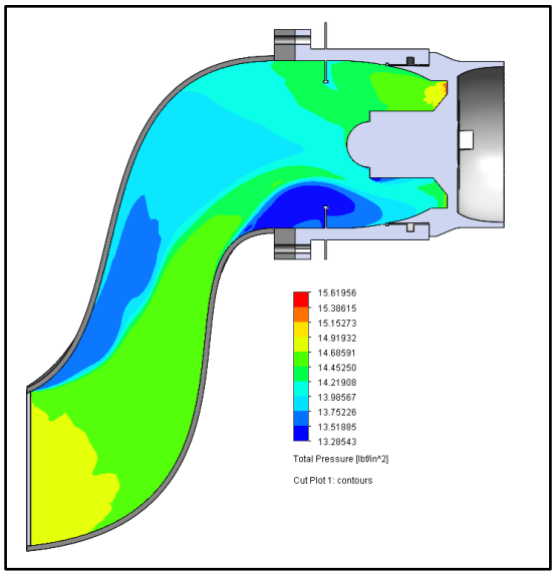

Figure 34: CFD Visualization (Flight Conditions) - Octagonal 6" (Iteration 2)

Goal Name	Unit	Value	Averaged Value	Minimum Value	Maximum Value
SG Average Total Pressure 1	[lbf/in^2]	14.69	14.69	14.69	14.69
SG Average Total Pressure 2	[lbf/in^2]	15.01	15.14	15.01	15.28
SG Average Total Pressure 3	[lbf/in^2]	14.18	14.55	14.17	14.93
SG Average Total Pressure 4	[lbf/in^2]	13.40	13.73	13.35	14.10
PiD_Inlet_Outlet	[lbf/in^2]	0.94	0.96	0.94	0.99
PiD_Inlet_Upper	[lbf/in^2]	0.96	0.99	0.96	1.02
PiD_Inlet_Lower	[lbf/in^2]	0.91	0.93	0.91	0.96

Table 3: Flight Conditions Recovery Data - Octagonal 6" (Iteration 2)

Another takeaway from these results is that, even with very high mach numbers, the pressure recovery shows very high percentages. The average values in the area where the kiel probes would be placed is about 99% on the upper probe and 93% on the lower probe. This is to be expected as the inlet curves back down into the transition duct and leaves an area of lower pressure right where the lower kiel probe would be. Although these results are not as promising as the static test inlet, they are still very high for the Mach Number range being tested. Since the flow will separate around the area of the lower kiel probe, a high recovery value is a good sign that the inlet is suitable for the mission.

X. Third Iteration

After the success of the second iteration, the team conducted one final iteration to decrease the inlet's volume while also keeping above the requirements set out by AFRL. This third and final iteration consists of an inlet 5.5 inches in axial length, a drop from the 6 inches of the first two iterations. The mouth area is the same as the second iteration, consisting of an octagon with 1.5 inch side lengths, resulting in an inlet area of 10.86 square inches. Models were run with this shorter axial length, a smaller mouth area, and both, but it was determined that decreasing the axial length was the best way to decrease the volume of the model while keeping the recovery value over the criteria specified by AFRL. The smaller mouth area created an adverse pressure gradient, where the pressure starts to push back out the inlet due to the gain in pressure as the air is siphoned up the inlet into the larger area. Decreasing the axial length served as the best way to limit the volume and avoid this issue. The model is shown below in Figure 35.

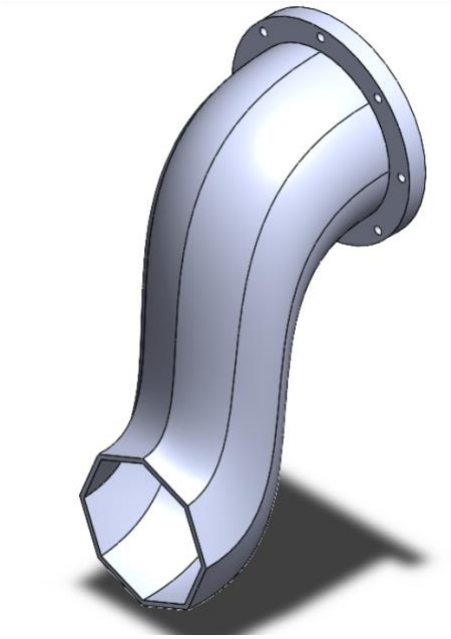

Figure 35: 5.5” Octagonal Inlet Model (Iteration 3)

As can be seen, this model is shorter than either of the previous models, and it does include a sharper transition from the lower inlet mouth to the upper outlet mouth. Below in Figure 36, the results are shown for this model’s upper probe, lower probe, and overall recovery are shown. These are then plotted with all previous octagonal models in Figure 36 to visualize the performance comparisons.

Parameter	Iteration 3 (5.5”)	Iteration 2 (6”)
Lower Probe pressure recovery	97.89%	99.75%
Upper Probe pressure recovery	99.23%	99.68%
Inlet/Outlet pressure recovery	99.09%	99.91%
Model Volume	21.8 in^3	22.3 in^3
Internal Volume	101.79 in^3	106.49 in^3

Figure 36: 5.5” Octagonal Inlet Model (Iteration 3) - Recovery Values

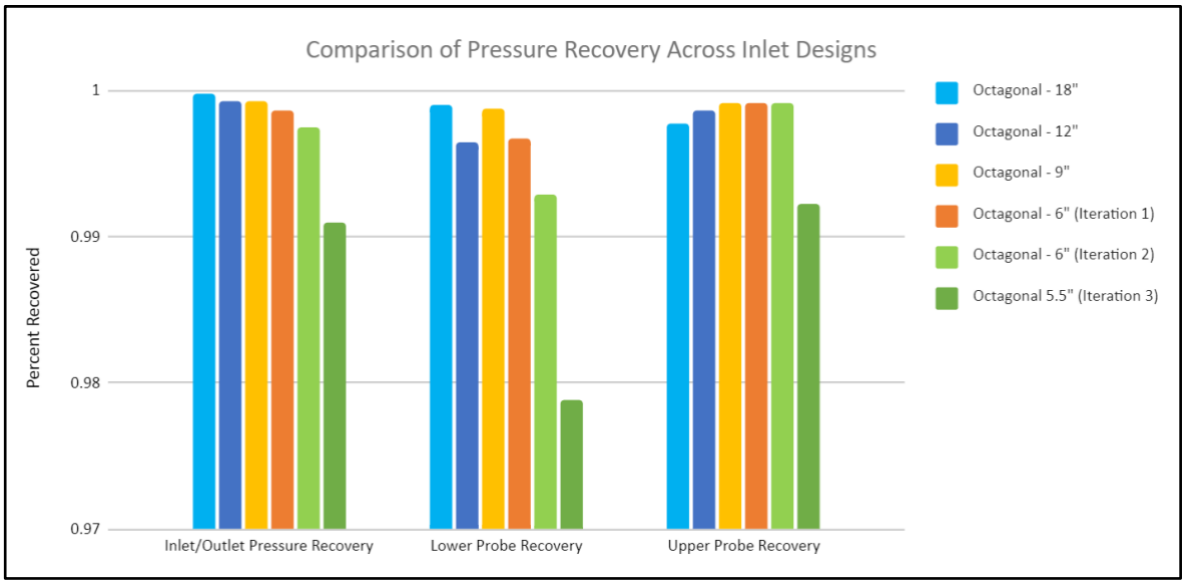

Figure 37: 5.5" Graphical Performance Comparison (All Octagonal Models)

To summarize, the team's third and final iteration showed an upper probe recovery value of 99.228%, a lower prove recovery value of 97.886%, and an overall recovery value of 99.094%. This is, clearly, the closest to the 2% pressure loss threshold. The team experienced a 0.23% loss from three refinements of CFD to actual testing for the first iteration's experimental testing. While the lower probe does exist in a lower pressure region with more than 2% pressure drop overall, the overall recovery is right around 99%, and the team does not expect more than a 1% pressure loss through friction. The CFD results are pictured below in Figure 38 and Figure 39.

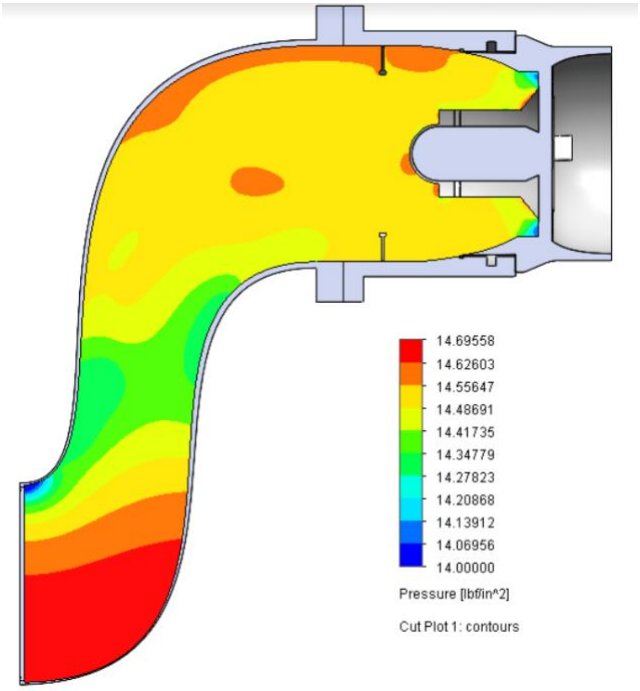

Figure 38: CFD Pressure Visualization - Octagonal 5.5" (Iteration 3)

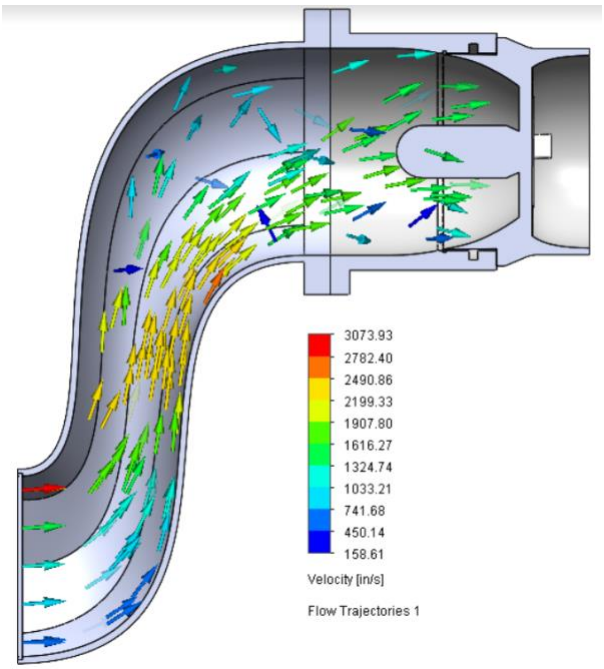

Figure 39: CFD Flow Visualization - Octagonal 5.5" (Iteration 3)

While the frictional losses cannot be known for either the second or third iteration without experimental testing, the team has been operating under the high estimate of 0.30% frictional losses to curb the design process once this was reached. While it is likely that this is an overestimate, it is necessary to take such caution as to not accidentally lose more pressure than allowed. While the expected effects of the boundary layer is increased, the boon from a decrease in surface area that causes friction may balance or possibly offset the increased effects of the boundary layer. The effect, though, cannot be determined without experimental testing. However, as the project is not able to be tested without a functional JetCat, the team finds this inlet sufficient in the project criteria and deems this inlet as the final iteration of the APOP Black Team's capstone project.

XI. Conclusions and Recommendations

Subsequent testing was planned, and a second iteration with promising CFD and a substantially smaller inlet volume was printed, sanded, primed, and painted. The team arrived with the intent to test with no inlet, test with the initial inlet, and test with the new inlet. Upon setup and purging the fuel, the team tried to run the JetCat, but the engine would not test. Batteries were swapped and charged, but there was no result other than smoke out of the engine. The ECU was thought to be the problem, since the compressor did not spin at all, and it was swapped with the other team's ECU. Still, there was no result but smoke out of the front of the engine. The team believes the starter is broken or not working properly, and no more testing can be done at the current moment.

As it pertains to future testing and a possible Phase II of the project, should it be renewed, the team has reached these conclusions and would like to give the following recommendations. The first inlet design with the idealized MFP sizing resulted in a pressure loss of around 0.23% and thrust loss of around 0.1%, which was well above what was expected when it came into factoring in real world conditions such as friction; this is believed to be due to the rigorous sanding and smoothing done to the inlet as well as the inlet having a small axial length and thus less friction can be achieved. The team believes that the ridges of the octagonal design served well to guide the flow and that the smaller inlet, which was ready to test, would have shown a similar, comparable result to the CFD and thus allowed for further iteration. It is the opinion of the team that shortening the axial length is a better way to

reduce model volume than to shrink the inlet area any further, as sharper turns do not seem to cause as detrimental an effect as an adverse pressure gradient caused by the pressure difference.

The overall consensus is that the inlet could be made much smaller than the one tested. This was reached during the experimental testing of the inlet that was first printed. However, the pressure testing was not available earlier in the testing phase, making it very difficult to iterate without further experimental testing. In this time, the initial concept was proven to have very little pressure loss. The next inlet was promptly printed and readied for testing. However, the morning of the test saw the engine experiencing technical difficulties and was unable to be tested. This made further data collection impossible and all data shown on this report is from the April 1st test. This was the first and last instance in which the pressure could be tested through the inlet concept.

Ideally, purchases made this semester are able to be reused and utilized by later teams, thus decreasing the need for allocation of the budget to tools and equipment. A backup JetCat purchase is something the team strongly recommends, as both JetCats - new and old - have experienced technical issues. For the Phase I of this project, it was deemed unnecessary to purchase a new engine for backup, but given that the project proved susceptible to such an unlikely occurrence of two engines, one new, failing within a week of each other, it is recommended that another is purchased.

The team's first inlet iteration was proven to succeed experimentally, with plenty of room for improvement. Though the experimental testing could not continue, the team's second inlet iteration decreased the volume of the first by greatly reducing the inlet's mouth area. The results for this iteration gave an idealized pressure recovery over 99.25%, with an expected actual recovery around 99%. The third and final iteration further decreased the volume by reducing the axial length by half an inch, which was shown through CFD testing to be the best way to decrease volume and keep the recovery over the 98% threshold. The recovery shows a 99.094% overall recovery. The team could foresee further improvements to keep flow attached at the lower probe to better reflect the overall recovery of the inlet. This iteration can be improved, and the team does not foresee over a whole percent of loss. The team defers all further improvements to future APOP teams. However, the team is confident in both the second and third models to perform as required while also giving AFRL models that are designed with the project requirements in mind. The team is also satisfied that they have delivered designs that limit the print volume and are easy to support, maintain, and manufacture. The APOP Black Team sees the project deliverables as more than sufficient and believes the project progress to be satisfactory to AFRL.

Appendices

Appendix 1: Procedures

I. All APOP Black Team Members are expected to follow the PPE guidelines in accordance with Oklahoma State University's COVID-19 protocols.

II. The team will aim to test once a week when conditions are favorable.

III. The team will ensure that the Test Stand and Engine are secure, that every screw is screwed tight each test, and that all FEA predictions are cleared before testing.

IV. The team will unlock the Test Stand's wheels and take it outside, via the ramp, and set up all the necessary power components.

V. The team will purge and connect the fuel line and make sure the fuel supply is sufficiently full and everything is sealed correctly.

VI. The team will connect the power to the test stand and ensure that the data acquisition software and transducers are connected and ready to collect data from the kiel probes and the loading cell.

VII. The team will put on the necessary eye and ear protection.

VIII. One team member will be ready to kill the power if needed, and one team member will have the fire extinguisher ready.

IX. The team members will clear the area of all small debris to ensure no engine ingestion issues.

X. The team will stand a safe distance away and begin data collection.

XI. The engine will be powered on and the rpm sequence will be run, as described above.

XII. The engine will be powered off and the data collection will be stopped.

XIII. The engine will be given three minutes to cool down.

XIV. The team will remove power from the system and disconnect the electronics.

XV. The team will carefully disconnect the fuel and ensure safe storage for the next test.

XVI. The team will safely disconnect all parts and ready the configuration for whatever tests need to be conducted in the future.

XVII. The team will return the Engine Mount inside, via the ramp, and lock the wheels once safely returned to the APOP room.

Appendix 2: Thrust Measurements

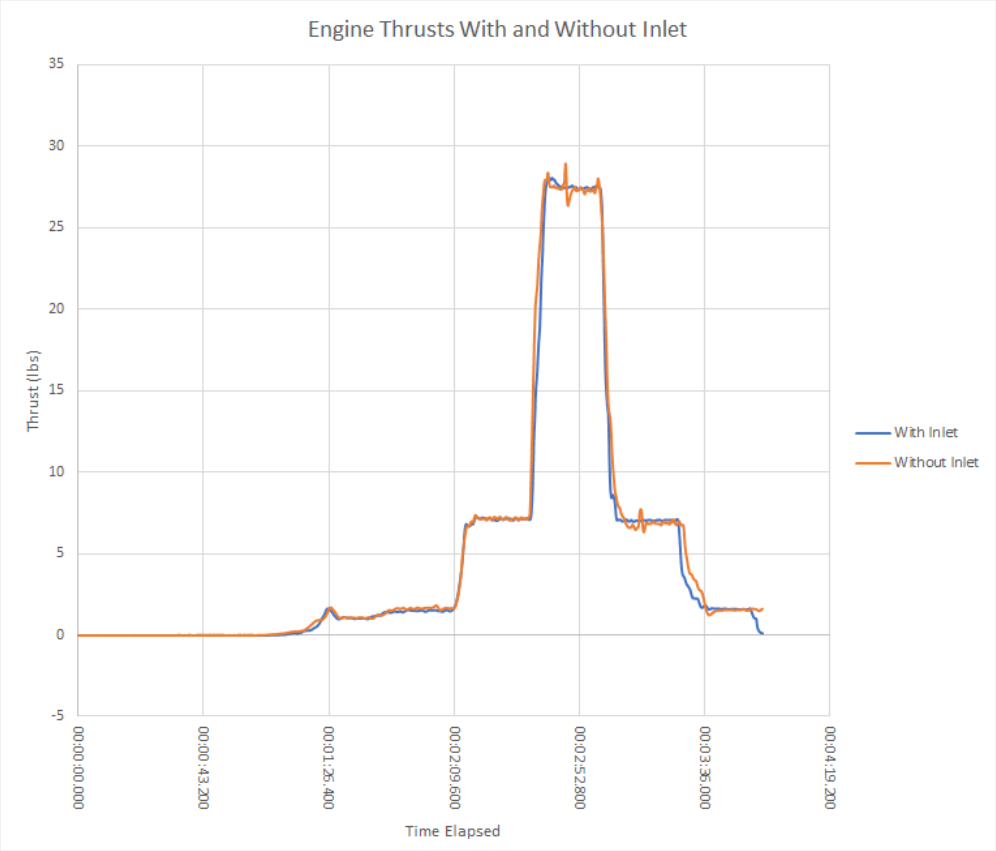

Appendix 3: Pressure Measurements

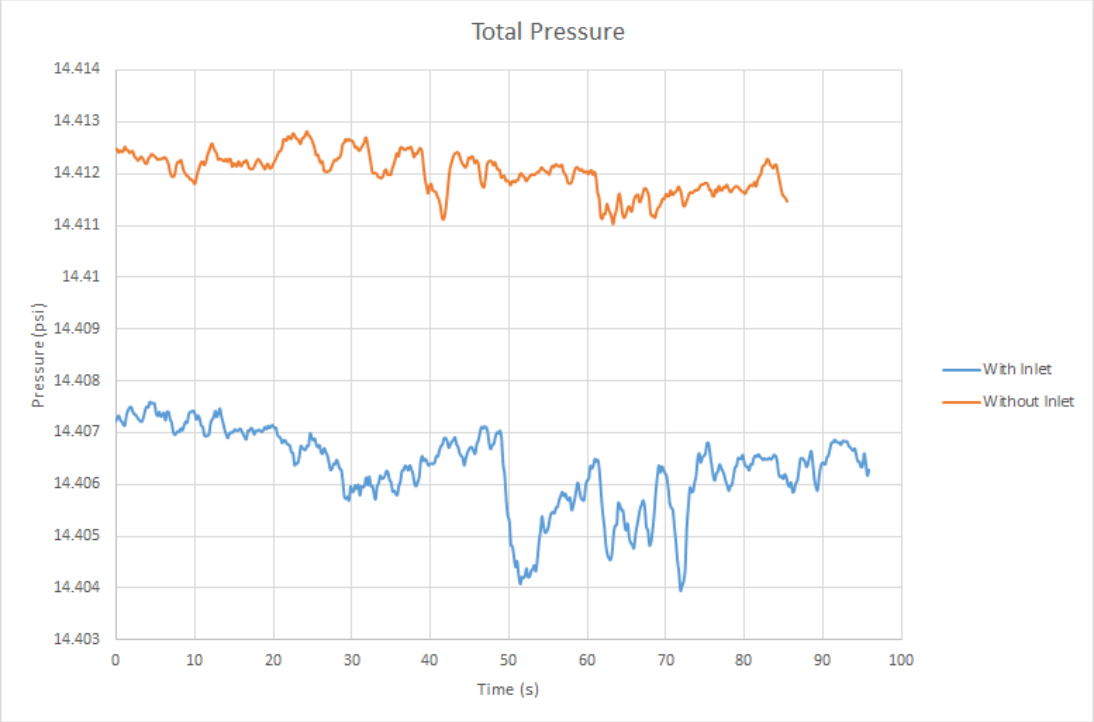

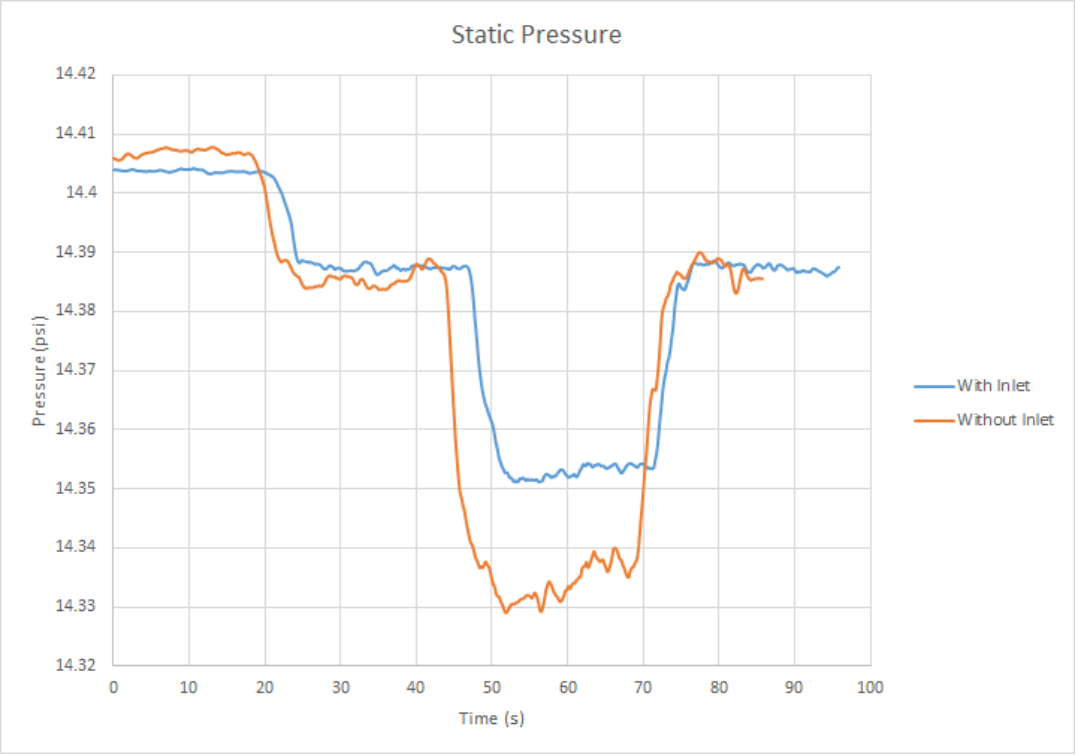

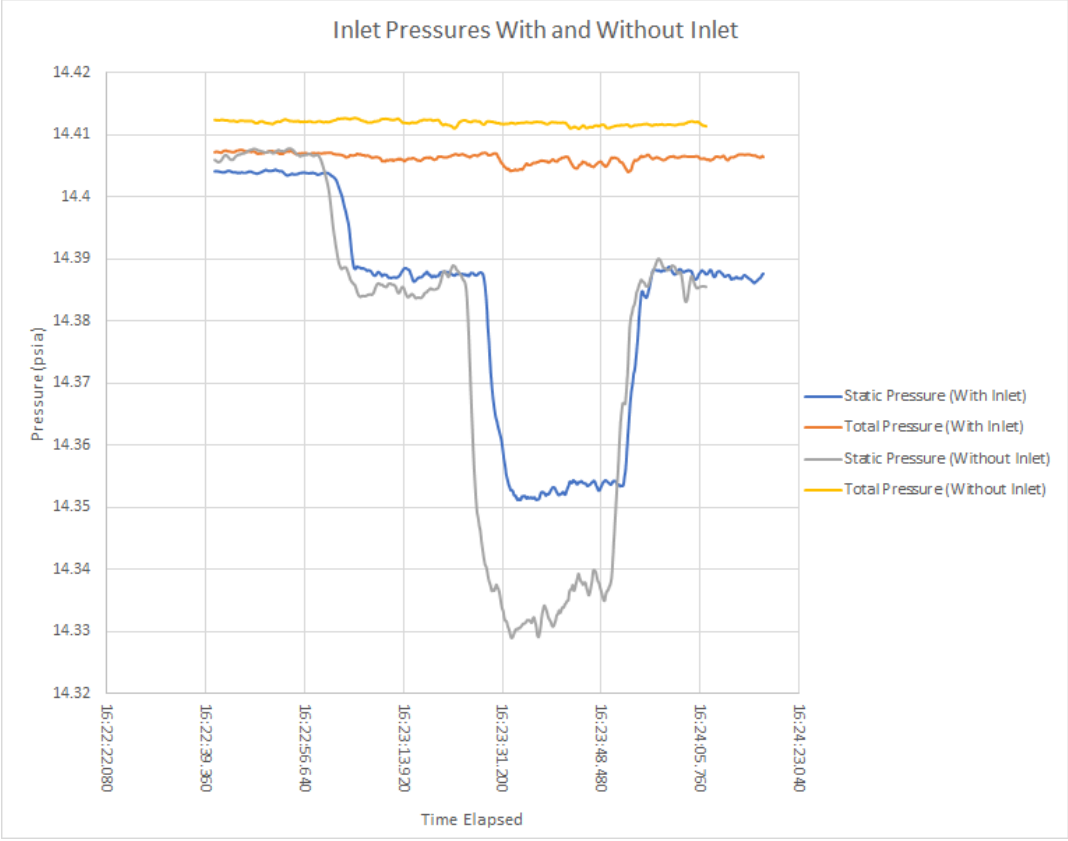
Inlet Pressures With and Without Inlet
14.42
14.41
14.4
14.39
14.38
14.37
14.36
14.35
14.34
14.33
14.32
Pressure (psisia)
16:22:22.080
16:22:39.360
16:22:56.640
16:23:13.920
16:23:31.200
16:23:48.480
16:24:05.760
16:24:23.040
Time Elapsed
Static Pressure (With Inlet)
Total Pressure (With Inlet)
Static Pressure (Without Inlet)
Total Pressure (Without Inlet)

Appendix 4: SFC Measurements

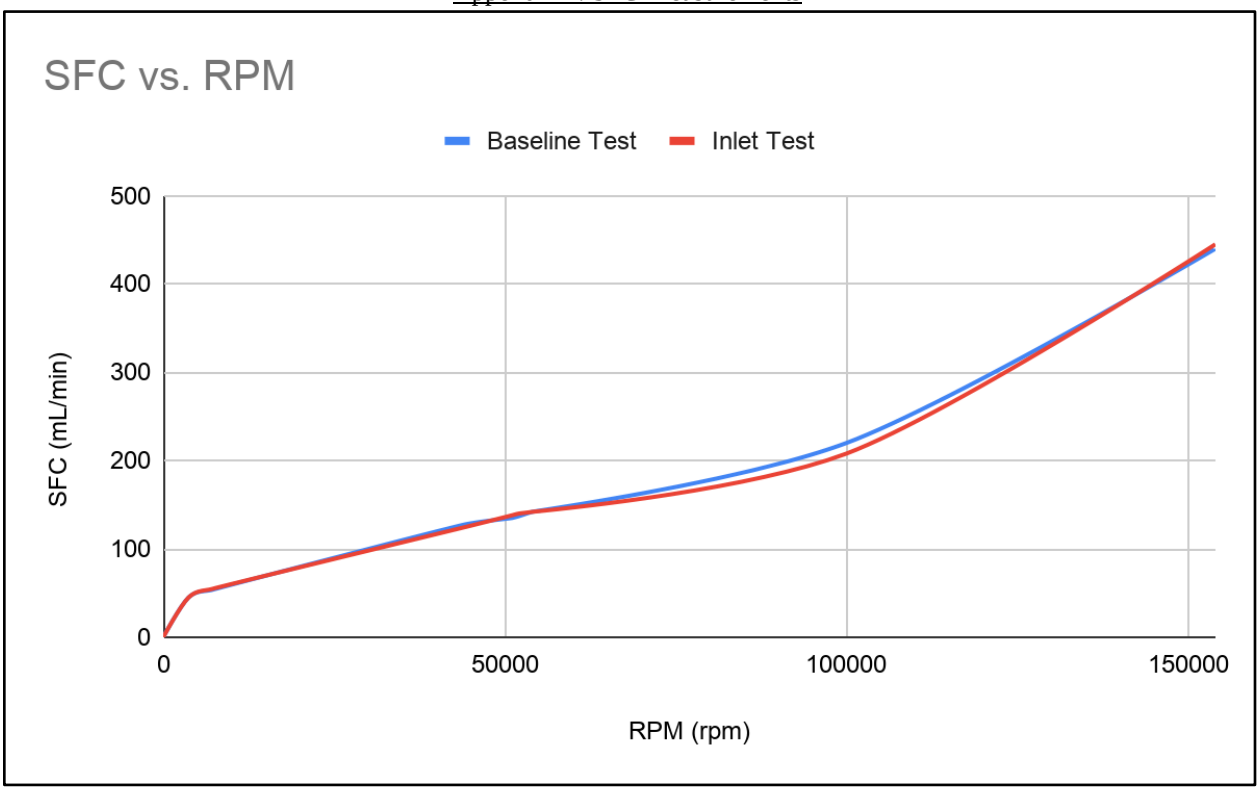

Sources

- Amazon.com: Online Shopping for Electronics, Apparel ... www.amazon.com/.
- APOP Statement of Work, provided by United States Air Force
- "AR Power 3400mAh LiFE Smart Balance Receiver Pack." Booma RC, boomarc.com/en/xs-power-3400mah-life-receiver-pack.
- Boston, University. "Important Announcement." *Mechanics of Slender Structures RSS*, 2021, www.bu.edu/moss/mechanics-of-materials-strain/.
- Dai, Houfu, et al. "Influence of Laser Nanostructured Diamond Tools on the Cutting Behavior of Silicon by Molecular Dynamics Simulation." *RSC Advances*, Royal Society of Chemistry, 9 Mar. 2017, pubs.rsc.org/en/content/articlehtml/2017/ra/c6ra27070k.
- "Department of Labor Logo UNITED STATES DEPARTMENT OF LABOR." Law and Regulations | Occupational Safety and Health Administration, www.osha.gov/laws-regs.
- Dr. Rouser, Daniel Velasco, Colton Swart
- eFunda, Inc. "Home." *Mechanics of Materials: Strain*, 2021, www.efunda.com/formulae/solid_mechanics/mat_mechanics/strain.cfm.
- Gerhart, Philip M., et al. Fundamentals of Fluid Mechanics. Wiley, 2020.
- "MAE 4010 Independent Research." Aerospace Propulsion & Power, aeropropulsion.okstate.edu/content/mae-4010-independent-research.html.
- Mattingly, Jack D., and Keith M. Boyer. Elements of Propulsion: Gas Turbines and Rockets. American Institute of Aeronautics and Astronautics, 2016.
- National Archives and Records Administration. "Electronic Code of Federal Regulations." *Electronic Code of Federal Regulations (ECFR)*, 10 Feb. 2021, www.ecfr.gov/cgi-bin/retrieveECFR?gp=&SID=7884ce6530725fcff55708ff45db627b&mc=true&r=SUBPART&n=sp36.3.1200.b.
- Papadopoulos, F., Valakos, I. M., and Nikolos, I. K., "Design of an S-duct intake for UAV applications," *ResearchGate* Available: https://www.researchgate.net/publication/242340760_Design_of_an_S-duct_intake_for_UAV_applications.
- Quellwerke, "P100-RX," *JetCat* Available: https://www.jetcat.de/en/productdetails/produkte/jetcat/produkte/hobby/Engines/p100_rx.
- Solidworks 3D CAD Software
- United States Air Force. *Air Force Research Laboratory*, 2021, www.afrl.af.mil/.
- VIccoo. "VIccoo Safety Glasses Personal Protective Equipment, PPE, Eyewear Protection, Clear High Impact, Vented Sides, For Construction." *Amazon.co.uk: Kitchen & Home*, 24 Mar. 2020, www.amazon.co.uk/VIccoo-Protective-Equipment-Protection-Constructio/dp/B086998HGB.
- "XS Power 2100mAh LiFE ECU Pack - MPX." Dreamworks Model Products - #1 in Radio Controlled

Jets and Accessories, www.dreamworksrc.com/xs-power-2100mah-life-ecu-pack-mpx.